AN-NAJAH NATIONAL UNIVERSITY
FACULLTY OF GRADUATE STUDIES

THE MELTING DYNAMICS OF NANOSCALE Pd CLUSTERS

A Molecular Dynamics Study Using the Modified Embedded Atom Method

By
SAJA IBRAHIM ABDUL-HADI

Supervisors
Dr. N.M.JISRAWI
BIRZEIT UNIVERSITY
Dr. M. ABU-JA'FAR
AN-NAJAH NATIONAL UNEVIRSITY

A Thesis Submitted in Partial Fulfillment of the Requirements for the Degree of Master of Science in PHYSICS, Faculty of Graduate Studies, At An-Najah National University, Nablus, Palestine.

2003

THE MELTING DYNAMICS OF NANOSCALE Pd CLUSTERS

A MOLECULAR DYNAMICS STUDY USING THE MODIFIED EMBEDDED ATOM METHOD

By
SAJA IBRAHIM ABDUL-HADI

This thesis was defended successfully on 2 March 2003 and approved by:

Committee Members	**Signature**
1. Dr. M. S. Abu-Ja'far (Associate professor)	.....
2. Dr. N. M. Jisrawi (Associate professor)	.....
3. Dr. Musa El-Hasan (Assistant professor)	.....
4. Dr. Marwan El-Kawni (Assistant professor)	.....

بسم الله الرحمن الرحيم

TO MY PARENTS

ACKNOWLEDGMENTS

First of all I would like to thank my supervisors Dr. Najeh Jisrawi and Dr. Mohammed Abu-Ja'far for their help, support and encouragement. Their guidance and great help made this work possible. Also I would like to present my thanks to the committee members: Dr. Musa El-Hasan and Dr. Marwan El-Kawni for their critical reading of this thesis and for their fruitful comments.

Special thanks go to the people who supported and helped me all along: Prof. Hikmat Hilal, Prof. Yousef Salamin, Mr. Abdul-Fattah Al-Batran, Dr. Isam Al-Ashqar, Dr. Adnan Yahya, and the staff of the physics departments in both An-Najah and Birzeit Universities.

Finally and most of all, I would like to thank my family for their support, encouragement and patience during all years of my study.

TABLE OF CONTENTS

LIST OF FIGURES

Number *Page*

Abstract

THE MELTING DYNAMICS OF NANOSCALE Pd CLUSTERS

A MOLECULAR DYNAMICS STUDY USING THE MODIFIED EMBEDDED ATOM METHOD

Clusters are systems of atoms that contain something between tens and tens of thousands of atoms. They form a link between individual atoms and the bulk, their finite size and large proportion of surface area, give them a special position in solid state physics. In this work, molecular dynamics simulations employing the modified embedded atom potential are used to study the melting properties of seven Palladium "Magic Number" clusters.

The clusters' behavior, change of structure, latent heat per atom, atomic positions, and melting temperatures of each cluster were calculated.

The most important results obtained in this work are: The calculation of the dependence of the melting temperature on cluster size. It is found that clusters have melting temperatures so much lower than of bulk that increase with the size of the cluster. The latent heat of fusion has the same behavior.

Melting does not occur at a specified temperature, but in a range of melting temperatures going from the outermost shells to the inner shells of the cluster.

In addition to this hysterisis in the transition temperature with cooling, the stability of the icosahedral structure is also studied.

Chapter 1

BACKGROUND

1.1 PARTICLE SIMULATIONS

Material Science investigations have traditionally been divided into experiment and theory. In the 20th century a third branch of science appeared: computational Science. In this branch of science computers are employed to simulate bulk materials, large or small systems of particles, and different atomic structures.

Today, particle simulation is a main method for generating information and analyzing the properties of systems.

1.1.1 A BRIEF HISTORY OF PARTICLE SIMULATIONS

Particle simulation techniques were developed in the 20th century coming to a good start in 1944 when John von Neumann was attracted to the ENIAC project (the world's first

operational electronic, general-purpose computer). He wrote a memo proposing a "stored-program computer". He believed: "Our present analytical methods seem unsuitable for the solution of the important problems arising in connection with nonlinear partial differential equations. The really efficient high-speed computing devices may provide us with those heuristic hints which are needed in all parts of mathematics for genuine progress." [1]

In 1953, the first Monte Carlo simulation of a liquid was performed by Metropolis, Rosenbluth, Teller, and Teller on the MANIAC computer at Los Alamos National Laboratory [2].

Enrico Fermi, John Pasta, and Stanislaw Ulam studied the dynamics of a one-dimensional array of particles coupled by anharmonic springs on the MANIAC in 1955.

Alder and Wainwright [3,4] studied the Dynamics of hard spheres (billiards) at the Lawrence Livermore National Laboratory in 1956 [5].

In 1960, Radiation damage in crystalline Cu was studied with short-range repulsion and uniform attraction toward the center by George Vineyard's group at Brookhaven National Laboratory and in 1964. The first simulation using interatomic potentials for a liquid (864 argon atoms) by Aneesur Rahman was done at the Argonne National Laboratory using a CDC 3600 computer [6]. In 1974, the first molecular dynamics simulation of a realistic system was done by Aneesur Rahman and Stillinger in their simulation of liquid water [7].

The history of the invention of interatomic potentials is interesting. It starts in the fifties, when Phillips, Kleinman and others invented the pseudopotential, followed in the sixties by the invention of the density functional theory (DFT), by Hohenberg, Kohn and Sham (1964-1965) [8].

A very significant theoretical improvement occurred in the 1985 when Car and Parrinello [9] showed how to use a group of algorithms developed for speed computations to calculate the

energies and forces between atoms, where atoms could be simulated using *Ab-initio* principles.

The Embedded Atom Method (EAM) was developed by Daw & Baskes (1983) [10] then developed for some fcc metals by Foiles, Daw & Baskes (1986) [11]. The Modified Embedded Atom Method potential (MEAM) by Baskes was developed for cubic metals (1992) and hcp metals (1994), Covalent Si and Ge (1989), Ni(1997) and Lennard-Jones based EAM (1999) [12,13].

1.1.2 THE TECHNIQUES OF MOLECULAR SIMULATION

Many molecular simulation techniques are available: Monte Carlo simulation (MC), the Molecular Dynamics simulation (MD), Molecular Mechanics Modeling, and the Static Lattice Modeling are different molecular simulation techniques, each of which has its own properties, and capabilities.

Molecular dynamics calculates the forces between molecules explicitly, and the motion is computed by solving Newton's equations of motion. From the initial positions, velocities and

forces, the position and velocity of an atom can then be calculated after a small interval of time.

Molecular Dynamics can calculate the details of structure (RDF, X-ray diffraction pattern, etc) as Monte Carlo can do, but the advantages of MD over MC is that it calculates and describes the molecular system as a function of time explicitly [14].

Monte Carlo generates the 'history' of the system of molecules, and calculates the bulk properties using statistical mechanics. It employs Random Walk routines (small random moves of the atoms in the system) to generate small pieces of atomic configurations. This works together with a sampling algorithm due to Metropolis et al., to make sure that the random walk will not go out of the thermodynamical configurations. The advantages of MC are that it is capable of making random moves, thus finding new properties. A known method such as Path Integral Monte Carlo (PIMC) is very successful in computing quantum system properties.

Molecular Mechanics modeling (MM) is a method that depends on the minimization of the potential energy function to compute complex molecular structures. Its advantage over MD and MC is that it is cheap.

Static lattice modeling (SL) depends on the method of minimizing of the potential energy function, and it uses minimization algorithms that collect the information based on the infrared spectrum of the lattice from the second derivative of the energy matrix. It differs from the MM method in that it is confined to periodic systems.

1.1.3 MOLECULAR DYNAMICS

1.1.3.1 THEORY

Molecular dynamics is "a powerful method for exploring the structure of solids, liquids and gases. Though a very modern method, requiring powerful computers, it would not have appeared strange to Isaac Newton. The idea is so simple; by

calculating the forces acting on the atoms in a molecular system and analyses their motion"[15].

We can study such systems under hard conditions, which can never be done by experiments, or solved by theoretical methods. This makes MD simulations an important part of a new branch of science called computational science.

We define molecular dynamics (MD) as "a computer simulation technique where the time evolution of a set of interacting atoms is followed by integrating their equations of motion"[16].

1.1.3.2 THE MATHEMATICAL MODEL

In molecular dynamics, we integrate Newton's second law (equation of motion) over time for each atom (or particle) in a system that contains N atoms to yield their positions and velocities.

$$\vec{F}_i(t) = m_i \vec{a}_i(t) \qquad (i = 1,\ldots,N) \qquad 1$$

In equation.1, the force $\vec{F}_i$ is the sum of all the forces acting on the atom i that results in the acceleration $\vec{a}_i$.

$$\vec{a}_i(t) = \frac{d^2}{dt^2}\vec{r}_i(t) \qquad 2$$

The force can then be written in the form

$$\vec{F}_i(t) = m_i \frac{d^2}{dt^2}\vec{r}_i(t) \qquad 3$$

$$\vec{F}_i = -\nabla V(\vec{r}_1,.....,\vec{r}_N) \qquad 4$$

$V(\vec{r}_1,.....,\vec{r}_N)$ is the total interacting potential energy function

$$-\frac{dV}{dr_i} = m_i \frac{d^2}{dt^2}\vec{r}_i(t) \qquad 5$$

Newton's equation of motion can relate the derivative of the potential to the change of position with time.

Finding positions and velocities after a small time interval (time step), then feeding them back again to recalculate the new position and velocities, this cycle is repeated again and again to construct what is called a full simulation (Figure 1), which takes

thousands of time steps. The time step taken depends on the type of system and material simulated and is in the femtosecond (10^{-15} second) range for the current Pd simulation. (Figure 1) summarizes the main steps done to get the results starting from the initial positions [17].

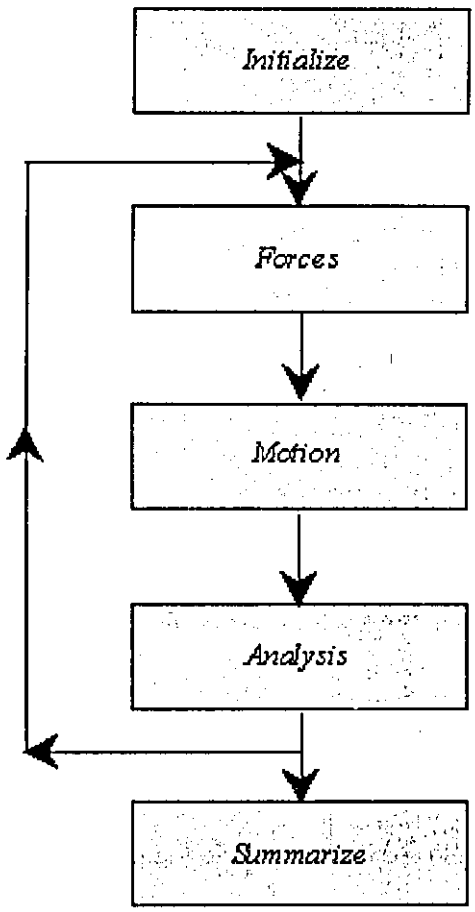

Figure 1 A Schemtic diagram illustrating the steps of a molecular dynamics simulation.

1.1.3.3 THE STATISTICAL MECHANICS OF MOLECULAR DYNAMICS

The thermodynamic state of a system can be defined by some simple parameters such as temperature, the number of atoms, pressure…etc. Other thermodynamic properties can be derived from the equation of state or the fundamental thermodynamic equations.

The aim of using statistical mechanics is to understand and predict macroscopic properties from microscopic or molecular information. Using molecular dynamics to measure quantities, means performing time averages of a property -which is usually a function of coordinates or velocities- over the system trajectory.

Any instantaneous physical property at a time t can be defined as:

$$A(t) = A(r_\tau(t), v_\tau(t)) \quad (\tau = 1,2,.....N_{tot}) \qquad 6$$

$$\langle A \rangle = \frac{1}{N_{tot}} \sum_{\tau=1}^{N_{tot}} A(t) \qquad 7$$

where τ is the time step number and N_{tot} is the total number of time steps.

The MD program calculates the sum $\sum_{\tau} A(t)$ and updates it at each step, but the average is taken at the end of the run.

This method is used to calculate all of the average instantaneous values, potential, kinetic and total energy, temperature, pressure, mean square displacement, stress, and other needed averages. Some of these quantities are discussed briefly here.

Potential Energy

The average potential energy ***V(t)*** is obtained at the same time as the forces are calculated by averaging the instantaneous values. We must not forget the dependence of the potential energy -and the forces- on the distances between the atoms.

In the MD calculation of the potential acting on an atom *i* by other atoms of the system, a distance called the cutoff distance

must be specified to determine the range of atoms that act on atom *i*, the forces by other atoms (out of that range) will be ignored, potential on atom *i* will be calculated only from those atoms inside that range. The cutoff distance for calculating the potential using MEAM method in this work is 5.34 angstroms.

Kinetic Energy

The instantaneous kinetic energy ***K(t)*** of the system depends directly on the velocity :

$$K(t) = \frac{1}{2}\sum_i m_i[v_i(t)]^2 \qquad 8$$

It is of course easier to calculate ***K(t)*** when the velocities $v_i(t)$ are determined. Averaging ***K(t)*** will give the average instantaneous kinetic energy.

The total energy is calculated by taking the sum of the kinetic and the potential energy :

$$E(t) = V(t) + K(t) \qquad 9$$

Temperature

The instantaneous kinetic energy ***K(t)*** of the system and the temperature ***T(t)*** are directly related and since the kinetic energy per degree of freedom is $K(t)=\frac{1}{2}Nk_bT(t)$ Here k_b is the Boltzman constant, and ***N*** is the number of atoms, then

$$K(t)=\frac{3}{2}Nk_bT(t) \qquad 10$$

By finding the velocity one can obtain the instantaneous temperature of the system.

Pressure

All the quantities in molecular dynamics are easily accessible except the pressure, which can't be obtained directly. In MD one makes use of the Clausius virial function $W^{tot}(\vec{r}_1,\ldots,\vec{r}_N)$ to obtain the pressure [16,18,19].

$$W^{tot}(\vec{r}_1,\ldots,\vec{r}_N)=\sum_{i=1}^{N}\vec{r}_i\cdot\vec{F}_i^{tot} \qquad 11$$

Where r_i is the position of atom i and F_i^{tot} is the total force acting on atom i. When averaging the Clausius virial function over the MD trajectory and using Newton's second law , we get:

$$\left\langle W^{tot} \right\rangle = \lim_{t\to\infty} \frac{1}{t} \int_0^t \sum_{i=1}^{N} \vec{r}_i(t) \cdot m_i \ddot{\vec{r}}_i(t)\, dt \qquad 12$$

Integrating by parts and using some simplifications, we can get a simple form of the average which is twice the kinetic energy

$$\left\langle W^{tot} \right\rangle = -2\left\langle K.E. \right\rangle = -3Nk_BT \qquad 13$$

If we think of the total force as external force plus internal force then the virial function is built of two terms

$$\left\langle W^{tot} \right\rangle = \left\langle W^{ext} \right\rangle + \left\langle W^{\text{int}} \right\rangle$$

For a parallelepiped sample of sides L_x L_y and L_z, the external part of the virial function is

$$\left\langle W^{ext} \right\rangle = L_x(-PL_yL_z) + L_y(-PL_xL_z) + L_z(-PL_xL_y) = -3PV$$

$$\left\langle W^{tot} \right\rangle - \left\langle W^{ext} \right\rangle = -3Nk_BT + 3PV = \left\langle \sum_{i=1}^{N} \vec{r}_i \cdot \vec{F}_i^{\text{int}} \right\rangle$$

This can be used to calculate the pressure P

$$P = \frac{Nk_BT}{V} + \frac{1}{3V}\left\langle \sum_{i=1}^{N} \vec{r}_i \cdot \vec{F}_i^{\text{int}} \right\rangle \qquad 14$$

Equation 14 reduces to the equation of the ideal gas for non-interacting atoms. This is how the pressure is calculated.

Many methods can be used for the pressure Control in a MD simulation [20]. Some are Berendsen method of pressure control, Andersen method of pressure control and Parrinello-Rahman method of pressure and stress control.

1.1.3.4 THE RADIAL DISTRIBUTION FUNCTION (RDF)

The radial distribution function [21,22] is a function that describes how the atoms are packed (radially) around each other or around one atom. This function is usually plotted as a function of ***r***, the interatomic separation, the mathematical formula that describes the radial distribution function RDF ***g(r)*** is:

$$\rho(r) = \rho \cdot g(r)$$

$$g(r) = \frac{n(r)}{\rho \cdot 4\pi r^2 \cdot \Delta r}$$

In which ***g(r)*** is the RDF, ***n(r)*** is the mean number of atoms in a shell of width Δr at separation ***r***, ρ is the mean atom density.

15

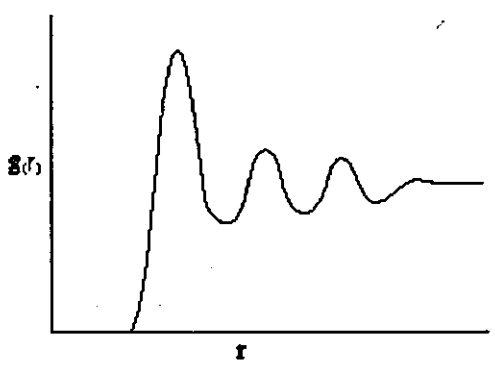

Figure2 g(r) the radial distribution Function as a function of r the radial distance.

The following are some of the features of $g(r)$:

*For small values of r, $g(r) = 0$ which is an indicator of the effective width of the atom.

*Peaks show the distances at which the atoms are highly packed in shells nearby each other.

*Sharp peaks show a high degree of order, in crystals for example, by increasing the temperature, thermal motion causes such peaks to disappear.

1.2 INTERATOMIC POTENTIALS

The forces in molecular dynamics simulations are derived from the equation of the potential energy, which is a function of the coordinates.

$$\vec{F}_i = -\nabla V(\vec{r}_1,.....,\vec{r}_N) \qquad 4$$

The potential energy function for a material $V(\vec{r}_1,.....,\vec{r}_N)$ must be specified to start MD modeling of that material, when we talk about the interatomic potential. We must remember that the Hamiltonian for a system of interacting atoms [16]is written as:

$$\hat{H} = -\sum_i \frac{\hbar^2}{2M_i}\nabla_i^2 - \frac{\hbar^2}{2m}\sum_\alpha \nabla_\alpha^2 - \sum_{i,\alpha}\frac{Z_i e^2}{r_{i\alpha}} + \sum_{i>j}\frac{Z_i Z_j e^2}{R_{ij}} + \sum_{\alpha>\beta}\frac{e^2}{r_{\alpha\beta}} \qquad 16$$

Where i,j refer to nuclei and α,β refer to electrons, M_i and R_{ij} are the masses and distances of nuclei, m and $r_{\alpha\beta}$ are of the electrons, Z_i the atomic number of nucleus i.

These terms are the detailed description of the equation:

$$\hat{H} = \hat{T}_N(R) + \hat{T}_e(r) + \hat{V}_{eN}(r,R) + \hat{V}_{NN}(R) + \hat{V}_{ee}(r) \quad 17$$

Where $\hat{T}_N(R)$, $\hat{T}_e(r)$ are the kinetic energies of the nucleus i and the electron α respectively. The other potentials $\hat{V}_{eN}(r,R)$, $\hat{V}_{NN}(R)$ and $\hat{V}_{ee}(r)$ refer to the electron-nucleus, nucleus-nucleus, and electron-electron potentials, respectively.

To solve Schrödinger's equation for the total wave function using this Hamiltonian without approximations is impossible.

In 1923 Born and Oppenheimer [16] found that nuclei are much heavier than electrons. The Born-Oppenheimer approximation depends on the fact that the nuclei are much more massive than the electrons, which allows us to say that the nuclei are nearly fixed with respect to electrons. We can then neglect the kinetic energy of the nuclei because $\hat{T}_N$ is smaller than $\hat{T}_e$ by a factor of M_N / μ_e, where μ_e is the reduced mass of an electron. Considering nuclei fixed, the above equation reduces to [23,24]:

$$\hat{H}_{el} = \hat{T}_e(r) + \hat{V}_{eN}(r,R) + \hat{V}_{NN}(R) + \hat{V}_{ee}(r) \quad (18)$$

$$\hat{H}_{el}\Psi(r,R) = E_{el}\Psi(r,R) \quad (19)$$

We can write the Schrödinger equation using the new Hamiltonian, and since R is considered as a constant which leads to a constant $\hat{V}_{NN}(R)$, then a new Hamiltonian without $\hat{V}_{NN}(R)$ of equation (18) will be only shifted by a constant.

$$\hat{H}_e = \hat{T}_e(r) + \hat{V}_{eN}(r,R) + \hat{V}_{ee}(r) \quad (20)$$

For a system of interacting atoms this must be solved to find the energy. Many models were suggested for the potential to find the total energy.

1.2.1 Two-Body Potentials

The Van der Waals interaction describes the interaction between the dipoles of two atoms, far from each other (the clouds of their electrons do not overlap), separated by distance

r. This is the suitable description of the interaction between the atoms of a noble gas, which has no chemical bonding.

The most commonly used two-body potential is the Lennard-Jones pair potential, which contains two terms ; a repulsive potential term of the form (a/r^{12}) produced as a result of the electron overlapping and the van der waals attractive term which can be written in the form ($-b/r^6$), the Lennard-Jones potential terms are described by the expression [16,25,26] :

$$\Phi_{LJ}(r) = 4\varepsilon[(\frac{\sigma}{r})^{12} - (\frac{\sigma}{r})^{6}] \qquad 21$$

r is the distance between atoms With ε and σ as the units of energy and distance respectively.

This potential was used widely [27-31] to investigate the properties of many clusters of materials, and noble gases.

1.2.2 MANY-BODY POTENTIALS:

Systems of atoms that contain a large number of atoms such as semiconductors and metals can't be modeled using the pairwise forces.

The most difficult are potentials for semiconductors as they have the loosely-packed diamond structure, which is the most stable when there is no pressure, but when pressure is applied, another structure will appear with more coordinates, and the liquids of the semiconductors are metals. For that and for many other reasons potentials for semiconductors are the most complicated.

The most popular models of potentials for the semiconductors are the Stillinger-Weber potential [16] which is a classical model, and the Tersoff [32] group of potentials, which depends on the bond order concept.

Metals are a special case, they are characterized by high electrical conductivity, and large numbers of electrons in the metal are free to move, as every atom has one or two free electrons.

A large contribution to the binding energy is due to the interaction between the ion cores of the metal and the conduction electrons. Metals usually crystallize in closely packed structures such as hcp, fcc, bcc ...etc [33].

The first understanding of the interatomic forces in simple metals was when pseudopotentials were introduced {example Cohen et al. (1971), Pettifor and Cottrell (1992)} [8], and remarkable progress was made to the many atom potentials when potentials based on the density or coordination concepts were developed for metals in the eighties. So many simplifications were used and analytical models are derived [8].

Examples of the potential models for metals are the glue model {Ercolessi, Parrinello and Tosatti (1988)} [34], Finnis-Sinclair potential {Finnis-Sinclair (1984)} [35], Effective medium theory

{Jacobson, Norskov and Puska (1987)} [36], and the embedded atom method {Daw and Baskes (1984), Foiles, Baskes, and Daw (1986)}[10,11].

A new form of EAM, the modified embedded atom potential MEAM was developed later. MEAM for covalent Si and Ge (Baskes, Nelson and Wright) was developed in 1989, for cubic materials and impurities in 1992 by Baskes [37], for hcp metals in 1994, for Ni in 1997, and in 1999 MEAM was developed based on Lender- Jones potential.

1.2.3 THE EMBEDDED ATOM POTENTIAL (EAM) AND THE MODIFIED EMBEDDED ATOM POTENTIAL (MEAM)

The embedded atom method treated each atom in the metal as an atom which is embedded into the electron gas created by other atoms (Figure 3).

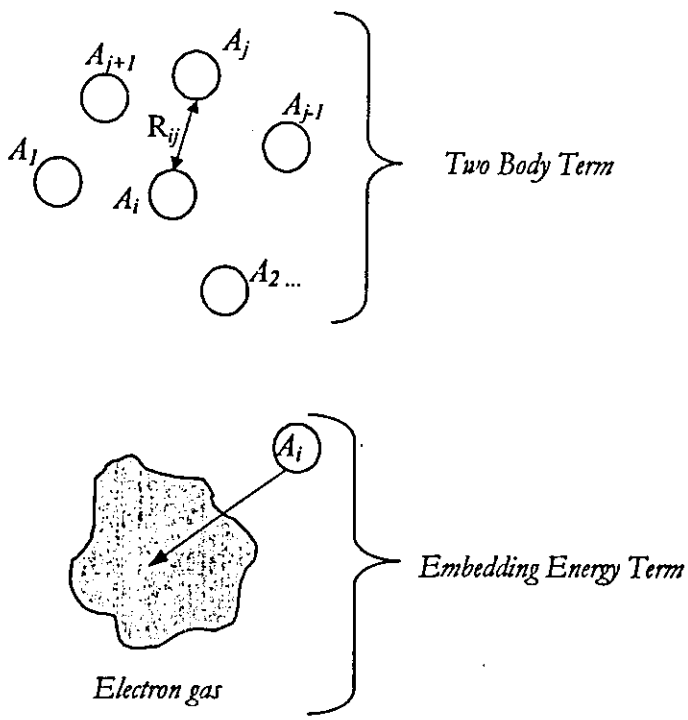

Figure 3 A schematic diagram illustrating the origin of forces acting on an atom A_i using the embedded atom method.

Working with the density-functional theory, the total electronic energy can be written as a function of the total electron density. In metals, we can use the approximation that the total electron density is the linear superposition of contributions from the individual atoms[11].

$$E_{tot} = \sum_i E_i \qquad 22$$

This gives a total energy, which contains two terms [12]:

Embedded energy term + Two body term

$$E_i = F_i(\overline{\rho}_i) + \frac{1}{2}\sum_{j(i\neq j)} \Psi_{ij}(r_{ij}) \qquad 23$$

Where $\overline{\rho}_i$ is the host electron density at atom i due to the remaining atoms in the system. It is also closely approximated by the sum of the atomic densities $\rho_j(r_{ij})$, which is the contribution to the density from atom j.

$$\overline{\rho}_i = \sum_{j(i\neq j)} \rho_j(r_{ij}) \qquad 24$$

This makes the total energy a function of the positions of the atoms r_{ij} [10].

$$\Psi_{ij}(r_{ij}) = \frac{Z_i(r_{ij})Z_j(r_{ij})}{r_{ij}} \qquad 25$$

$\Psi_{ij}(r_{ij})$ is the core-core pair repulsion between atom i and j separated by a distance r_{ij}.

Finding the energy depends on the calculation of F and ψ. They are calculated in detail in {Daw and Baskes (1984)} for nickel and palladium, and in {Foiles, Daw and Baskes (1986)} for the fcc metals Cu, Ag, Au, Ni, Pd, Pt, and their Alloys.

Later the modified embedded atom method MEAM for covalent Si and Ge {Baskes, Nelson and wright} was developed in 1989. Baskes also calculated the MEAM for cubic materials and impurities in 1992 [37], for hcp metals in 1994, for Ni in 1997, and in 1999 MEAM was developed based on Lender-Jones potential.

The difference between EAM and MEAM is that the EAM considers spherical symmetry, where $\bar{\rho}_i$ is given by a linear superposition of spherically averaged electron densities, while MEAM includes ***s, p, d, f*** symmetries, here $\bar{\rho}_i$ is augmented by a term that depends on the angular parameters ***s, p, d, f***. In the calculations of MEAM, (1992) Baskes calculated the potential for ten fcc, ten bcc, three diamond cubic, and three gaseous materials by considering the case of homogeneous monatomic solid with interactions limited to first neighbors[37].

The embedding function F_i used in the MEAM is a function of electron density ρ

$$F_i(\rho) = A_i E_i^0 \rho \ln \rho \qquad 26$$

Here E_i^0 is the sublimation energy and A_i is the scaling factor for the embedding energy, the total background density can be formed by taking a weighted sum of the squares of the partial densities:

$$(\overline{\rho}_i)^2 = \sum_{l=0}^{3} t_i^{(l)} (\rho_i^{(l)})^2 \qquad 27$$

Where $t_i^{(l)}$ is the weighting function, $t_i^{(0)}$ is taken to be equal to unity. The atomic electron densities $\rho_i^{a(l)}$ are assumed in the form:

$$\rho_i^{a(l)} = \exp\left[-\beta_i^{(l)}\left(\frac{R_{ij}}{R_i^0} - 1\right)\right] \qquad 28$$

The parameter $\beta_i^{(l)}$ is the exponential decay factor for the atomic density, l=(0-3) for (***spdf***) and R_i^0 is the equilibrium nearest-neighbor distance.

In his paper, Baskes determined all the parameters E_i^0, A_i, $t_i^{(l)}$, $\beta_i^{(l)}$ and R_i^0 for the cubic materials to calculate the MEAM energy [37].

The embedded atom method was used as it is or with some modification to study bulk metals [38], metallic alloys [39], metallic clusters [40-43], metallic nanowires [44], and metal foams [45].

1.3 ATOMIC CLUSTERS

1.3.1 DEFINITION

Clusters are small systems of atoms, which contain anywhere between tens and tens of thousands of atoms. Their properties are different from these of atoms and molecules or those of the bulk.

Metallic clusters were known since the middle ages. They were used to color the stained glasses. This was noticed by Rayleigh, then followed by Mie (1908) who treated it electro dynamically [46]. Since those days clusters have been investigated.

The special position of clusters in solid state physics is not only because of their finite size, large proportion of surface atoms, and loss of transnational symmetry, but also because of their energies. It's known that atoms have discrete energy levels while bulk materials have bands of energy levels. Clusters are an

interesting case, since clusters are positioned between atoms and the bulk.

Metal clusters are very important. Their importance from a technological point of view came from their role as catalysts in important chemical reactions.

If we take a closer look at the clusters' structures we will see that the larger clusters prefer to have spherical surface structures similar to that of bulk, like the Cuboctahedral structure of clusters of the face centered cubic (fcc) metals, while smaller clusters prefer the less energetic structures such as icosahedrons and dodecahedrons [40].

1.3.2 SIMULATED CLUSTERS

In recent years, the simulation of clusters was the subject of a large body of research, as the thermodynamical, structural and other properties of clusters were studied. Different clusters: (with different potentials, structures, size...etc) were investigated and many different techniques were used: (first

principle method *[ab-initio]*, molecular dynamics, Monte Carlo ...etc).

As an example, the Cambridge Cluster Database [31] contains tens of such simulated clusters, using classical or quantum simulation programs.

1.3.3 MAGIC NUMBERS (THE CASE OF PALLADIUM)

Palladium, like other fcc metals have the Cuboctahedral structure for the larger clusters. The Cuboctahedron is a structure of atoms that has six square faces and eight triangular faces. Although this structure is constructed from close-packed layers, the square faces reveal a surface that is not closely – packed [47].

For small Cuboctahedral clusters, it is favorable to transform to the icosahedral structure which has a five-fold symmetry structure [48] with lower energy [44]. In the Pd cluster, this can be noticed for clusters with less than 15000 atoms or a cluster of 7.4 nm diameter [41].

In the Icosahedral structure, a five-fold symmetry structure that is found in small clusters, where the surface to volume ratio is proportionally high, the atoms are closely packed to create complete shells of 20 triangular faces. In the shells, the shell-to-shell interatomic distance is smaller than that between atoms of the same shell.[47] (Figure 4)

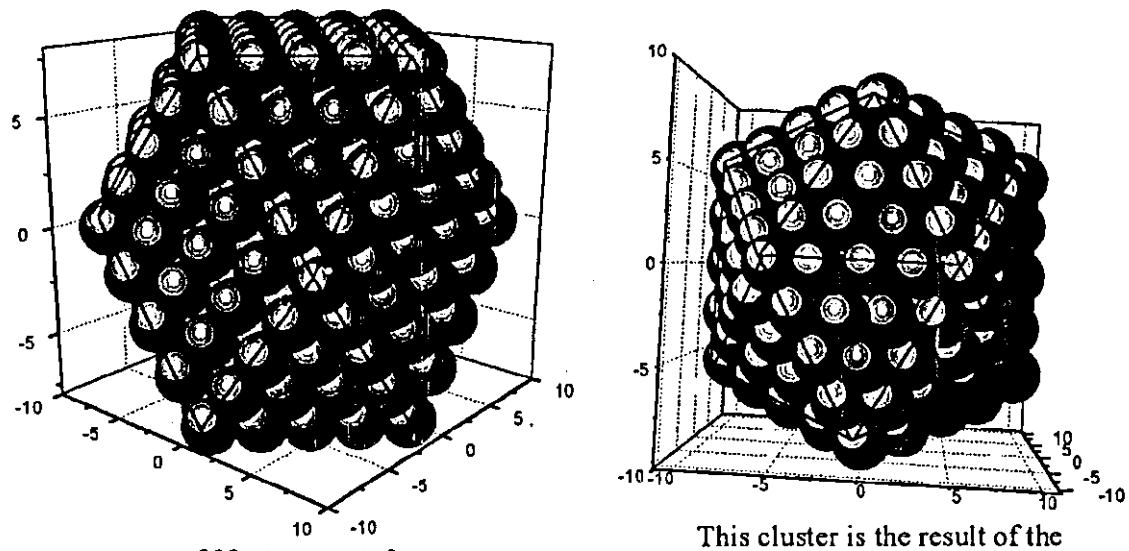

Figure 4 The three dimensional view of the 309 atom cluster before and after the conversion from Cuboctahedral to Icosahedral structure.

The Icosahedral structure is a favorable structure according to the surface to volume ratio of atoms. It is formed for small

palladium clusters (up to 147) at room temperature, while for larger clusters; a higher temperature is needed to initiate the transformation [41].

The MacKay's Icosahedron [49] is an excellent example for the shell structure. The number of atoms in the surface k shell is

$$Ns = 10\kappa'^2 + 2 \qquad \kappa' = 1, 2, 3....$$

Where $(\kappa' = k-1)$, the total number of atoms n in k shells according to Mackay is:

$$N(k) = \frac{10}{3}k^3 - 5k^2 + \frac{11}{3}k - 1 \qquad 29$$

$k = 1, 2, 3...$

The clusters that have these numbers of atoms are closed, their shells are completely filled, and these numbers are called magic numbers. Both the Icosahedral and the Cuboctahedral structures are shown in Figure 5.

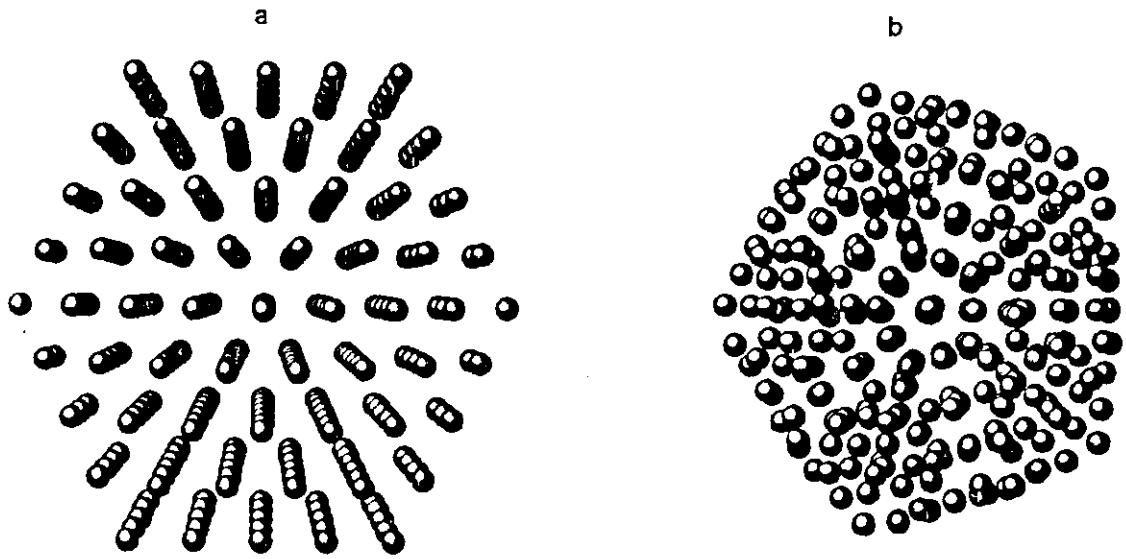

Figure 5: 309 Atoms in both (a) the Cuboctahedral structure generated using Latgen0 for 309 atoms and (b) the Icosahedral structure which was produced at the end of the simulation at 300K.

In table 1, the number of atoms added according to the shell index *k*, the number of subsurface and total number of atoms in the closed shell cluster are calculated, and the ratio of the number of surface to volume atoms and in the cluster.

Table 1 The total number of atoms contained in *k* closed shells, with the added atoms according to the increase of *k*, and the ratio of the number of surface to volume atoms .

Shell Index *k*	1	2	3	4	5	6	7	8	9	10	11	12
New added atoms N_S^*	1	12	42	92	162	252	362	492	642	812	1002	1212
N_{SS}^*		1	12	42	92	162	252	362	492	642	812	1002
N_C^*			1	13	55	147	309	561	923	1415	2057	2869
Total No. of atoms N_v	1	13	55	147	309	561	923	1415	2057	2869	3871	5083
Ratio $\frac{N_S}{N_V}$ %	100	92.3	76.4	62.6	52.4	44.9	39.2	34.8	31.2	28.3	25.9	23.8
Ratio $\frac{N_S + N_{SS}}{N_V}$ %	100	100	98.2	91.2	82.2	73.8	66.5	60.3	55.1	50.7	46.9	43.6

***Ns* :number of surface atoms, *Nss* : number of subsurface atoms, *Nc*: number of "core" atoms and *Nv*:total number of atoms in the cluster.**

1.3.4 METALLIC BEHAVIOR OF CLUSTERS

The development of metallic behavior of the cluster as a function of cluster size divides the clusters into three cluster size regimes: small, medium and large cluster. [50]

Table 2 Johnston's division of the clusters according to their size, the third column was found for the icosahedral clusters of magic numbers.

Cluster size	Number of atoms	Ratio of surface atoms $\frac{N_s}{N_v}$ for magic cluster included in the regime*
Small	$\leq 10^2$	≥68%
Medium	10^2 - 10^4	20 % - 68 %
Large	$> 10^4$	< 20 %

***According to figure 6, where the size of the clusters depends on Johnston regimes.**

With such division, Johnston discussed the development of metallic behavior in clusters, with an assumption of the spherical shape of the clusters, so that the radius of the cluster of N atoms $r = r_{ws}N^{1/3}$, r_{ws} is the Wigner-Seitz radius. Figure 6 shows the ratio of the surface atoms of the cluster with the radius of the cluster r, to illustrate the relation between the

cluster properties and the high ratio of surface atoms, the figure is divided into (Johnston) three cluster size regimes.

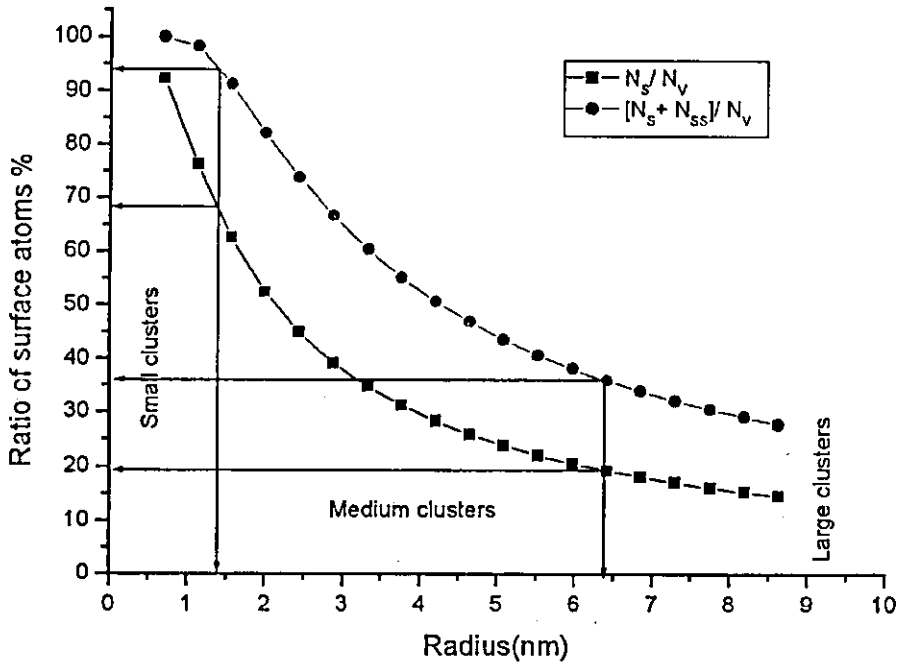

Figure 6 The ratio of surface atoms plotted with the radius of the cluster, the circles are for the ratio of surface and subsurface atoms $\frac{N_S+N_{SS}}{N_V}$, the blocks are for the ratio of the surface atoms $\frac{N_S}{N_V}$, the diagram is divided according to the three cluster size regimes.[1]

The description of the energy of the metallic cluster, changes with changing the size of the cluster.

---

[1] The radii are from reference 41(Jisrawi, N.M. Critical size for the cuboctahedral to icosahedral structure phase transition in nanometer-sized Pd clusters (unpublished).

As the cluster size (or the number of atoms) increases, the electronic energy levels become similar to that of the bulk. The cluster has more "metallic" properties than the smaller clusters. Figure 7 shows a schematic diagram for the changes of the electronic energy levels with increasing the size of the metallic cluster.

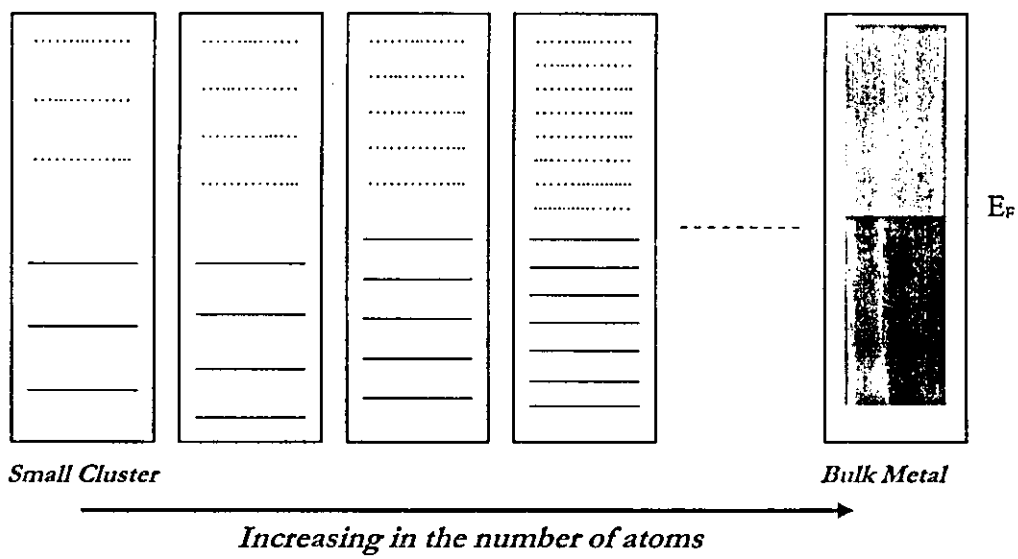

Figure 7 A schematic diagram of the electronic energy levels with increasing the number of atoms at 0K, where the doted lines are for empty levels and the full lines for filled levels. Ef is the Fermi energy.

For large clusters, many cluster properties that depend on the size of the cluster (depend on the radius of the cluster ***r*** or the number of atoms ***N***) such as the melting temperature,

ionization energy…etc, act "regularly" with increasing the size. For medium and small clusters, some deviation in this regularity occurs because of the quantum size effect, which is not included in this work.

Properties such as the melting temperature, ionization energy, binding energy and cohesive energy, can be described using simple laws [47, 50] as a function of r or N:

- $Y(r)$ is a cluster property that is a function of r the radius of the cluster.

$$Y(r) = Y(\infty) + \alpha r^{-1} \qquad 30a$$

- $G(N)$ is a cluster property that is a function of N the number of the atoms in the cluster

$$G(N) = G(\infty) + \beta N^{-\frac{1}{3}} \qquad 30b$$

It is found that the cluster parameters as a function of the number of atoms in the clusters have extremum values at magic numbers of atoms [28].

1.4 MELTING

The melting temperature of the bulk has been investigated widely and for along time. The so much used and famous metals (gold, silver, copper, aluminum ...etc) were investigated. Experiments and simulations were done to find the melting temperatures, the surface melting [51], the latent heat of fusion, the changes of the structure due to melting and cooling, and the dependence of the melting temperature on the potential [38].

The clusters' melting temperature T_m is so much lower than that of the bulk [47,52,53]. The melting temperature depends on the cluster's size [29,54], structure and surface area [55]. Melting starts from surface shell [28] because atoms have fewer nearest neighboring atoms than the inner atoms, this means less binding energies [55].

With a magic number of atoms, the icosahedral structure has a closed outer shell (no vacancies are found in the structure), which has to be more stable explaining the need for a larger amount of heating to get over the bond strengths.

1.4.1 THE MELTING OF METALLIC CLUSTERS (Na, K, Sn, Cu, Au, Ni, Pd)

A lot of metallic clusters were the subject of investigation. Some of these will be discussed below to give a clear idea about the melting behavior of metallic clusters in general. Some of the results mentioned below are experimental; others are the result of simulation.

When discussing the results of the melting of metallic clusters, it was noticed that clusters have a melting temperature below that of the bulk [52,53,56,57].The temperature of melting and the latent heat of fusion increase when the cluster is larger. While Bulk melts at a well-defined temperature, clusters melt over an interval of temperatures [28,58,59], which increases as the

cluster size decreases [60]. Clusters can fluctuate in time between being completely solid or liquid [58,60]. Clusters melt gradually as energy increases and the melting goes from outer to the inner shells [28,29,61-63].Metallic clusters have large proportion of atoms on the surface that have a very different electronic environment from atoms in the interior [60].

For very small clusters, T_m decreases with the cluster size. This was noticed for very small clusters with less than 50 atoms. [56] For example {($T_{m(Cu_{13})}$=1350K) > ($T_{m\ (Cu_{55})}$=975K)[61] and for Na with number of atoms below 90 [57], and $Sn_{(15\text{-}35)}$ melts 50K higher than the bulk [52]}.

It is much easier for the cluster to go from an ordered state to disordered state. This is why, upon quenching, large hysterisis at the transition temperature was observed [28,42,43]. When freezing the clusters, large facets are present, because of the finite time limitations of MD simulation (incomplete transition to the ground state).

Most of these results agree with this work, the properties of all the metallic clusters are similar, and if there is any disagreement, then this must be because of a special case (property) for that metal.

CHAPTER 2

TECHNIQUE AND METHODOLOGY

In this chapter, a description of the techniques used to do the actual simulation are briefly discussed. We will do this at the level of discussing the details of how the input and output files are made, how the code to generate the initial position of the Cuboctahedral cluster atoms runs, how the embedded atom potential file is prepared, the input files for the molecular dynamics simulation program used (XMD)[2] are created, and including a detailed description of the XMD simulation program.

We will also discuss how the generated output data files for the melting of palladium clusters are interpreted. How the energy, atomic positions and the radial distribution functions are created and analyzed.

---

[2] http://www.ims.uconn.edu/centers/simul/#xmd

2.1 THE BUILDING OF CLUSTURS

Here is a brief description of the code that was used to generate the position of the atoms in the Cuboctahedral palladium lattices.

Written by Christian Sachs, Latgen0.cc (Appendix II) is a c++ code that generates the Cuboctahedral lattices. The size of the cluster is specified according to the shell index k as defined in section (1.3), table 1.

The seven clusters have magic numbers with closed shells, with k varying from k=3 to k=9. The results are palladium clusters of Cuboctahedral structure that contains of 55, 147, 309, 561, 923, 1415, and 2057 atoms. These clusters have the same lattice constant as that of bulk fcc palladium. Immediately after the simulation, the lattice constants were adjusted to reflect energetics of the cluster structure.

Many quantities are included in the code (such as the lattice separation, Boltzman constant, atomic number .....etc), most of these quantities are specified for the element in this work, which is palladium.

2.2 SOFTWARE FOR MOLECULAR DYNAMICS SIMULATIONS

A large number of molecular simulation software programs are available on the public scientific websites. Some are for classical simulations (MC, MD…), others are for quantum simulations (*Ab Initio*). Some of those software programs are for a specific system, others are more general. Bulk, clusters, molecules, noble gases, metals, semiconductors, crystalline materials, polycrystalline materials…etc are subjects of investigations. The most popular MD programs are discussed, with a brief description to compare there capabilities, and to know what each one is specialized of in table 5. (Appendix I)

Although writing one's molecular dynamics code is not impossible and a host of popular texts tell you exactly how to do that, we opted for the choice of using a popular program used by a computational science group.

The chosen program is XMD which is a program that performs computer molecular dynamics (CMD) simulations on metals and ceramics, on personal computers (PC's).

2.2.1 THE SIMULATION SOFTWARE: XMD

XMD is a program developed by Jon Rifkin at University of Connecticut[3] for performing molecular dynamics simulations, using simple Pair, EAM, Tersoff Carbon-silicon, or Stillinger-Weber Carbon potential [64]. It is designed for the simulations of metals and ceramics. This software is written in C , can easily be used under Linux. It has the capability to read and write the data in text format, generating the energies, positions, velocities, forces, temperature, pressure, volume...etc for individual atoms and the averages of the whole system. Besides, the speed of the

---

[3] This software and associated documentation can be obtained from the website of the university of connecticut's group of Professor P.Clapp and J. Rifkin:
http://www.ims.uconn.edu/centers/simul/#xmd

simulation for a PC is acceptable. For example, the simulation of the 561-atom palladium cluster at melting temperature for 200000 time step (500ps) takes about 77 minutes , while it takes 17 minutes for 147 atom cluster , and 380 minutes for the 2057-atom cluster on a 550 MHz Intel Pentium III PC with 128Mb of RAM running Open Linux .

Using XMD, specific lattice structures can be generated, and calculations can be preformed statically and dynamically.

The XMD software was used (by Benjamin J. Soulé de Bas [39]) to study the diffusion process in ordered B2 compounds at high temperature using an embedded atom interatomic potential developed to fit NiAl properties. Nam, Hwang, Yu, and Yoon [43] used XMD to investigate the formation of an Icosahedral Structure during the Freezing of gold nanoclusters (Surface-Induced Mechanism) using the embedded atom potential. A study of meta-stable sites in amorphous carbon lattice generated

by rapid quenching of liquid diamond with Tersoff's empirical potential [65] was done using XMD.

2.2.1.1 THE PROGRAM

The XMD program actions are controlled by some commands that are read from one or more text files. In fact, all the input, output, and recorded data during the simulations are normal text files.

The initial positions and velocities of the atoms are specified, and using the potential the forces are calculated, then using these positions, velocities, and forces, and a small time interval, which is called time step, we can find the new positions and velocities which are the new input of the simulation. Repeating that for thousands of time steps (each a fraction of a picoseconds) we can generate some information about the energies, positions and velocities of the atoms.

We used the XMD in this work to find the melting temperatures for palladium clusters. The way of preparing the

input files and collecting the output data files is described below.

2.2.1.2 THE INPUT AND THE OUTPUT FILES OF XMD

The XMD program was used for the melting simulation of the palladium clusters using the Modified embedded atom method. The input files, output files, and the needed data files are text files. The EAM file was created using the XMD and the used potential is from the potential by Baskes et. al[4]. In the input files of XMD, the potential must be written or can be read from another file by the READ command.

XMD can simulate only a finite number of atoms, so when a relatively large number of atoms need to be simulated, as in bulk samples, the usual technique is to resort to periodic boundary conditions in the three directions. This way, when an

---

[4] The potential was downloaded from the website communicated to us privately by Professor M. Baskes. We would like to thank him greatly for his help.

atom gets out of the box through a wall, another atom comes in through the opposite wall.

If the repeating boundary conditions are off in one direction, the result will be a simulation for an infinite sheet of atoms, if it is off in two directions, an infinite wire of atoms will be simulated.

To do the integration of the Newtonian equations of motion for the atoms over a small time interval, the user of the XMD must specify this time interval which we call the time step. We can find the optimum time step using the XMD [66] but we have used a timestep for the Pd simulation which is compatible with the time scale of relaxation time for thermal processes, namely about 50 fsec.

In XMD, the sample is molted by placing it near a heat reservoir and waiting for its energy to change. We use the Canonical Ensemble (NVT): This is a system whose

thermodynamic state is characterized by a fixed number of atoms, N, a fixed volume, V, and a fixed temperature, T.

The temperature needs to be controlled during the melting simulations. This is done by taking the initial positions of the atoms as known, the temperature as known, but random velocities are assigned by XMD using appropriate Maxwell-Boltzman distribution for the specified temperature. Controlling the temperature is done by the ITEMP command. The instantaneous kinetic energy ***K(t)*** of the system depends directly on the temperature and since the kinetic energy per degree of freedom is $K(t) = \frac{1}{2} N k_b T(t)$ then:

$$K(t) = \frac{1}{2}\sum_i m_i [v_i(t)]^2 = \frac{3}{2} N k_b T(t) \qquad 31$$

Here k_b is the Boltzman constant, and N is the number of atoms. According to equation 31, if we determine the temperature, the velocities can be easily estimated.

To maintain an approximately constant temperature, the CLAMB command is used to scale the instantaneous velocities of the particles by $\left[\frac{T}{temp}.\left(\frac{1}{2\cdot cstep}\right)\right]$ to let the temperature go to the required value.

The temperature T is the instantaneous system temperature, *temp* is the appropriate temperature, and *cstep* is a parameter that controls how fast the algorithm converges.

The output that can be generated by XMD consists of atomic coordinates, velocities, energies, atomic stress, radial distribution function (RDF), and many other related parameters. In our work, we generate the data for the coordinates of each atom, average energies of the clusters, and the RDF for the clusters along the running simulation. Of course they are generated as tables in text files.

2.2.1.3 USING XMD IN THE BUILDING OF CLUSTERS

Some structures can be built using XMD. Many examples are included in the manual, such as filling a sphere of some radius, or creating a diamond cubic lattice, or bcc or fcc lattices of the same or different types of atoms for each. Lattices with the atoms filled in a specific orientation can be also created.

2.2.1.4 USING XMD FOR CREATING AN EAM POTENTIAL FILE [67]

The Embedded Atom Potential file can be built in text form as a set of tables, using the information about the potential units, the type of potential, the types of atoms. The EAM potential for Pd was adapted for XMD from Baskes [PRB 46, 2727(1992)] It can be stored as a separate file to be read by any XMD simulation input file of palladium.

The EAM file can be built according to the information and the examples [67] in the XMD manual:

```
# This is an example XMD potential file
#
eunit eV
potential set eam 2
#
potential pair 1 1 10 0.0 5.0
900.0  800.0  700.0            <---
600.0  500.0  400.0            <--- -- This is the
original table
300.0  200.0  100.0  0.0       <---
#
potential dens 1 10 0.0 5.0
900.0  800.0  700.0
600.0  500.0  400.0
300.0  200.0  100.0  0.0
#
potential embed 1 20 0.0 1000
```


Using this information the potential input file for Pd has been made as follows:

```
#EAM potential for Pd
#Adapted by Najeh Jisrawi from the potential by Daw et.al.
# Date Jun 29, 2000
eunit eV
potential set eam 1
#
potential pair  1   1   499  0.01070707105  5.34282827400
1.30512640600E+05
6.35500546900E+04
.
.
9.33401196300E-08
0.00000000000E+00
0.00000000000E+00
#
potential dens 1 500  0  5.342828274
0.00000000000E+00
-5.02766442900E-06
.
.
1.52897555900E-07
0.00000000000E+00
0.00000000000E+00
```

```
#
Potential embed 1 500 0 0.25
0.00000000000E+00
-3.13067108400E-01
.
.
-1.57194576300E+01
-1.57236957600E+0
```

This potential is applied to the cluster to calculate the forces, which leads to collect the information about the positions and the velocities of atoms.

2.3 GENERATED DATA FOR THE MELTING OF Pd CLUSTERS.

2.3.1 ENERGIES

The energies output text data file is generated by XMD using the commands –ESAVE- which writes the CMD (computer molecular dynamics) time step number and the energies in a file:

```
esave nskip filename.e
```

nskip tells the program how many CMD time steps should pass before it writes the energy. The energies written are the total energy, the potential energy and the kinetic energy. These energies are the average energies per atom.

If the needed energies are the energies for each atom the command -Write …EATOM- will write the indices and the energies for each atom or the selected atoms:

```
write FILE filename.e EATOM
```

An example for the energy data collected using the esave command is the energy file for the Pd_{55} cluster at 300K written using the line

```
esave 100 +Pd55_300.e
```

The output file looks like the following:

```
100 3.112599e+00 -3.148953e+00 +3.635339e-02 +0.00000e+0
200 3.123657e+00 -3.169412e+00 +4.575472e-02 +0.00000e+0
300 3.156116e+00 -3.206916e+00 +5.079960e-02 +0.00000e+0
.   .            .             .             .
.   .            .             .             .
.   .            .             .             .
```

The average energies are saved every 100 CMD time step. The total energy per atom is used in our calculations to find the melting temperatures.

2.3.2 Atomic Positions

The XMD input file causes XMD to read the initial positions using the READ command, the forces are applied to these atoms, the positions of the atoms change according to the integration of Newton's equation over a CMD time step, then

the atoms are in their new positions. Repeating this many times and saving the new positions at the time specified by the user using the - write ...PARTICLE- command, the resulting file will contain the types of the atoms and their positions.

Here is an example (a few lines from the Pd_{55} file) containing the READ initial positions command and the write ....PARTICLE command:

```
read pd55pos.dat
.
.
.
write FILE 55_800_5.pos PARTICLE
```

The output file for the positions of atoms contains the types of atoms and their x,y, and z positions.

```
PARTICLE        55
     1      0.0287     -2.4357     -4.6068
     1      2.0318      4.2339      0.8865
     1     -2.0486      2.5539     -5.0202
     .      .           .           .
     .      .           .           .
     .      .           .           .
```

Those positions are then used to draw pictures for the cluster during the melting process

2.3.3 DENSITY DISTRIBUTIONS

As was discussed in section (1.5), the structure of the cluster can be understood using the radial distribution function RDF. Any change in the structure can be recognized using the RDF too.
In this work the RDF used gives the number of atom pairs with a given separation. The XMD software writes a table of the radial distribution function, which is a histogram of the number of atom pairs between a given range of separations. The quantity ***g(r)dr*** given is the number of atom pair that are within ***dr*** of a distance r from each other. The XMD command to write the RDF is

```
write FILE filename.* RDF nbin rmin rmax
```

where rmin and rmax are the minimum and maximum values of separation in angstroms and nbin is the number of data bins.

As an example, the command line used to write the RDF for the Pd55 cluster at 800K during the simulation is :

```
write FILE 55_800_5.out RDF 25  0  15
```

A few lines of the output file resulting from this command are:

```
RDF  25  0.000000  15.000000
0.30      0      0
0.90      0      0
1.50      0      0
2.10      6      6
2.70    191    197
3.30     40    237
.        .      .
.        .      .
.        .      .
```

Each line has three numbers on it, the first is the value of the separation at the center of the bin, the second is the number of atom pairs in that bin, and the third is the sum of the atom pairs for all the above bines [64].

The radial distribution function for each cluster was recorded 10-20 times during a melting simulation. Figure 8 is only meant to illustrate what these RDFs look like. It shows the interatomic

separation for a magic cluster, at the beginning, during, and after the melting.

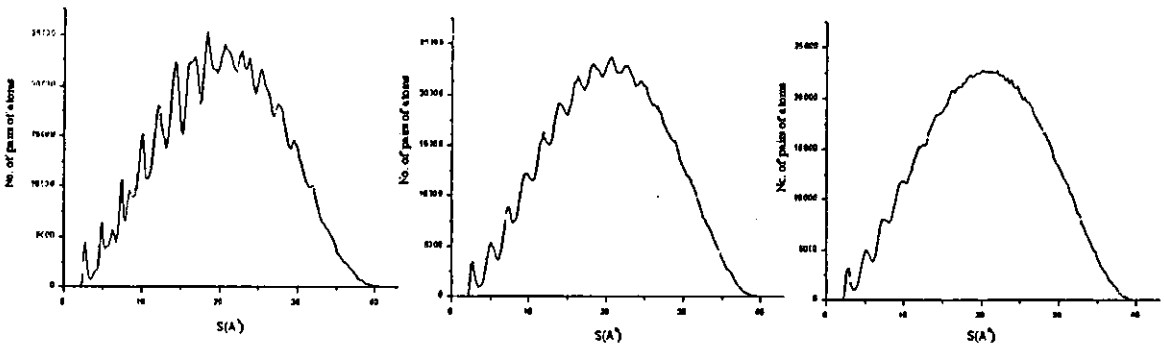

Figure 8 Radial distribution functions (RDFs) for Pd….. , at the beginning, during, and the end of the melting process.

CHAPTER 3

RESULTS: THE MELTING DYNAMICS OF MAGIC NUMBER PALLADIUM CLUSTERS

3.1 INTRODUCTION

Clusters have different properties from those of the bulk. Their shape, their limited number of atoms, the relatively large number of surface atoms and the relatively large surface area are the main causes of these differences. When investigating clusters, we must expect results that are so much far from the properties of the bulk, but the asymptotic behavior has to lead to bulk values.

In this chapter, a detailed discussion and analysis of the results is done.

The main results of this work can be summarized as follows:

1. The melting temperatures of the clusters are lower than that of the bulk.

2. The melting temperatures increase with the increasing size of the cluster. The asymptotic value for the melting temperatures leads to the "simulated" melting temperature for the bulk.
3. The latent energy of fusion also increases with increasing cluster size.
4. Cuboctahedral palladium clusters with magic numbers of atoms at melting temperatures go into the same scenario to reach melting: they convert to icosahedral clusters before melting. But since the melting occurs over a wide range of melting temperatures, this conversion does not have the same result:

- For lower temperatures of the melting range, the resulting Icosahedron atoms are much in order, the icosahedron looks so much similar to the perfect icosahedron, and the melting occurs after a nearly complete conversion.

- For higher temperatures of the melting range, the atoms of the icosahedron are so much disordered, the outer shells are more ordered, while the inner are not. Melting occurs before the complete conversion.

5. The stability of the clusters with magic numbers is evident. The magic number clusters need longer time to melt than clusters of other configurations (completely closed shells).
6. The Icosahedron with magic numbers is also more stable at higher temperatures. At temperatures higher than the melting temperature T_m, the Icosahedron takes longer time than that needed for the Cuboctahedron with the same number of atoms to melt.
7. At the melting temperature T_m, the Icosahedron melts earlier, because of the time needed for the Cuboctahedron to convert to an Icosahedron.

8. Hysterisis at the transition temperature was noticed after cooling the melted cluster. This was investigated in more detail for Pd_{147}.
9. As is now known from other studies [52, 56, 57, 61], the melting temperature of very small clusters is much higher than expected. We have investigated this for Pd_{13} which has a very high melting temperature in comparison with larger clusters.

These results are analyzed and discussed in details in the next section.

3.2 RESULTS

Even though Palladium in both bulk and cluster form was the subject of numerous simulation studies, the number of studies of the melting properties of "magic-number" clusters has been rare.

The melting behavior of small palladium clusters, with numbers of atoms n in the range ($12 \leq n \leq 34$) has been the subject of the study by Y.Lee, E.Lee, S.Kim and R.Nieminen.[29] They "show that the potential energy distribution of atoms in the clusters can consistently explain many of the important phenomena which occur during phase changes of small clusters, such as the nonmonotonic variation of melting temperature with the size of clusters" [55]. They calculate the melting temperature of Pd_{13} to be around 820K. This is of course potential dependent but we will show below that much higher values are obtained for the EAM potential in use here ($T_m(Pd_{13})>1200K$).

The melting temperature of the "magic number" palladium cluster, Pd_{55}, was determined by Grönbeck, Tomànek, Kim and Rosén [68] to be between 950K-1070K in their study of Hydrogen induced melting of Palladium clusters using the Many-Body-Alloy (MBA) Hamiltonian and the pairwise repulsive Born-Mayer interaction. In the current work it was determined to be 750K. Several other studies tackled other properties of Palladium clusters. [40,41,69,70].

A particularly interesting study is the work by Wolf, Mansour, Lee and Ray [38] in which they try to determine the temperature dependence of the elastic constants of embedded-atom models for palladium. The melting temperature of palladium metal, was determined using four different embedded atom potentials, with different elastic constants, and compared with the experimental value 1825K.

It was noted by the authors that the latent heat calculated using the EAM models was so much lower than the experimental value.

The results of this thesis are consistent with results for the bulk palladium; most of those results are summarized in table 3.

Table 3 Summary of various studies on the melting properties of bulk Pd. In this table we compare our results with those of other EAM based investigations. The experimental value of the melting of palladium is 1825K.

Potential	Melting temperature of the bulk [38](K)[a]	Latent heat (KJ/mol)	Latent heat (meV/atom)
EAM (Foils, Daw and Baskes)	1480[a] 1390[b]	7.79[a]	80.7
EAM (Voter)	1588[a] 1520±150[c]	9.96[a]	103.2
EAM (PDW3)[a]	1728[a]	10.2[a]	105.7
EAM (PDW5)[a]	1828[a]	9.84[a]	102.0
Results of this work [Figures 12,16 and 17]	1399	~7.12 8.99	~74 93.2
Experimental	1825	16.7[d]	173.1

a Wolf, Mansour, Lee, and Ray work using many types of embedded atom potentials (PDW3), (PDW5) are two methods developed by this group.
b Foiles and Adams, from the pervious reference.
c Ercolessi and Voter, from the pervious reference.
d Iida and Guthrie, from the previous reference.

The melting temperature of the bulk determined above are acceptable in comparison with the results of Foiles and Adams, but lower than the one by Ercolessi and Voter or the one by Wolf, Mansour, Lee, and Ray.

A result that comes out very clearly from the table is that the melting temperature determined by the simulation is so much lower than the experimental value.

The latent energy per atom for the bulk is also determined from the figures. It is lower than the experimental latent energy, and the latent energy from the work of other groups. But as mentioned by Kluge, Ray and Rahman and noticed by others, the latent heat determined using the EAM potential is so much lower than the experimental value [38].

3.2.1 MELTING TEMPERATURES OF CLUSTERS

How can we specify the melting temperature of a cluster? Generally, different method are used to indicate melting, some use the mean square displacement as a function of time, or

radius, in which the ordered shells can be easily realized. Others use the caloric curve, where a jump in energy indicates the absorption of latent heat. Those indicators are usually used to specify the melting temperatures.

In this work, we plot the total energy per atom (E_{tot}/atom) versus time for each cluster at different temperatures. We can specify a region of temperatures where the melting occurs for each cluster. It is found that if the reservoir temperature is close enough to the melting point of the cluster and one can wait long enough, the system flips to the energy associated with the liquid state. In this work, the melting point of a cluster T_m is defined as the temperature at which the cluster flips into the liquid state within a temporal simulation window of between 100ps and 400ps. This window is basically chosen arbitrarily to satisfy the criteria that one has waited enough but not too long.

We begin our discussion of the melting simulation results by considering in Figure 9, a plot of (E_{tot}/atom) vs. time for the

Pd_{2057} cluster. The melting appears as a "jump" in the energy with the height taken to be equal to the latent energy for the melting.

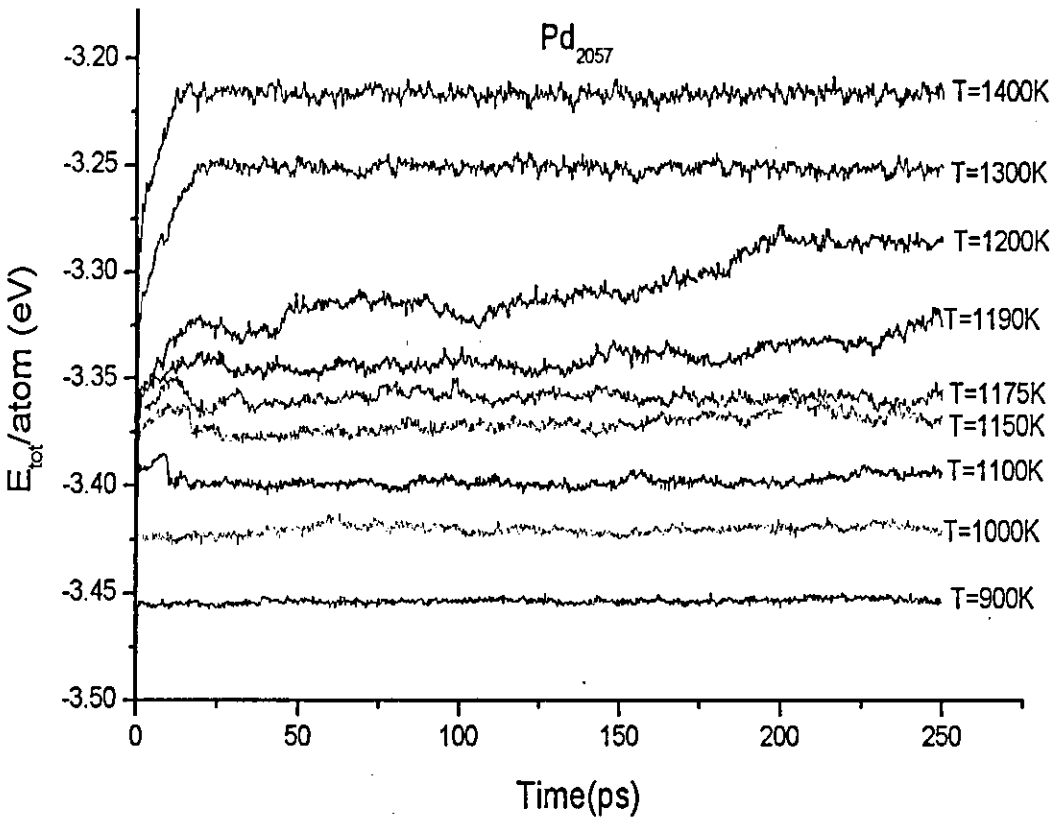

Figure 9 The total energy per atom vs. time for Pd_{2057} cluster at nine different temperatures, the melting is observed clearly at 1200K

We can specify the melting region also by plotting the average E_{tot}/atom vs. temperature for all the temperatures that the cluster is simulated at as in Figure 10 and we can calculate the

latent heat of fusion (per atom) for the cluster at the melting temperature, which appears as a step in the energy with a height ΔE.

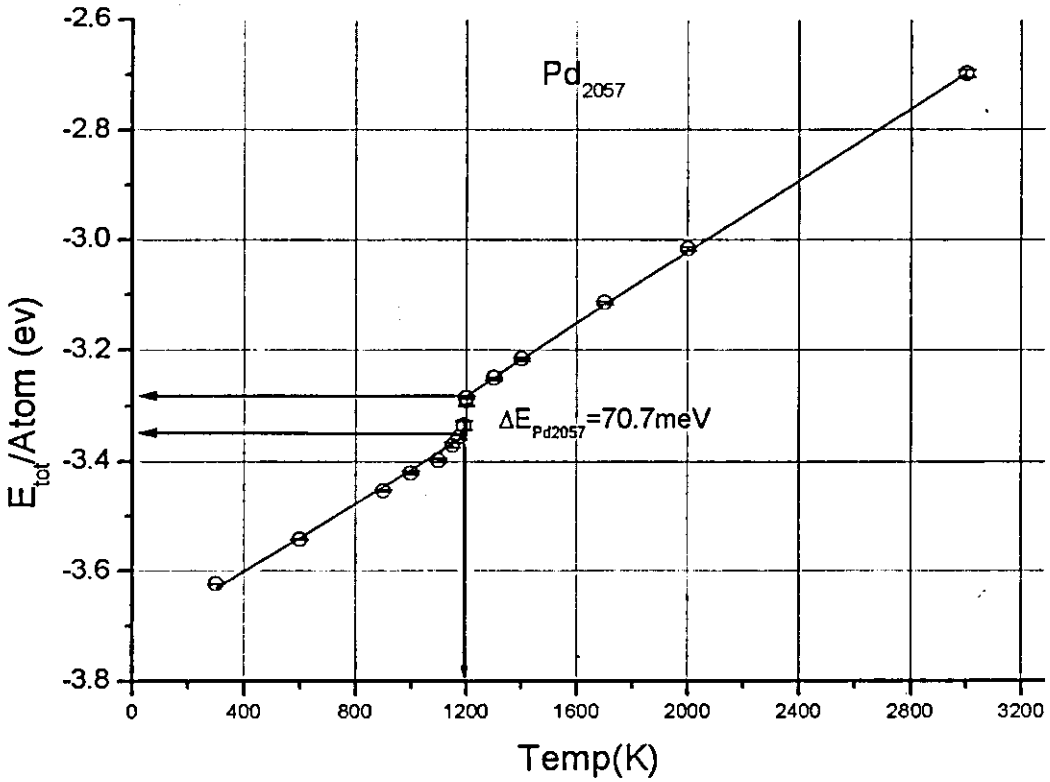

Figure 10 The total energy per atom vs. Temperature for Pd_{2057}. The melting is observed clearly at 1200K, and the latent energy ΔE is calculated.

Here, the uncertainty in E_{tot}/atom at a certain temperature came from calculating the standard deviation (SD) of the large number of total energy data points at that temperature.

The melting temperatures T_m and the latent energy per atom ΔE for the seven simulated clusters are generated as described and the results are summarized in table 4.

Table 4 : The melting temperatures and the latent energies per atom for the seven simulated clusters

N atoms	55	147	309	561	923	1415	2057
T_m (K)	750	910	1050	1100	1145	1175	1200
ΔE -latent energy per atom- (meV)	26	44	58	62	67	69	71

The generated results for the seven melted palladium clusters, using figures plotted for the clusters, similar to figures 9 and 10.

Since the melting occurs at a region of temperatures around T_m, this region is used as the uncertainty of T_m.

The results of the melting temperatures and the latent energy per atom in table (4) show a direct dependence of these two quantities on the size of the cluster. As a new shell is added to the cluster, an increase in melting temperature and the latent energy occurs. Plotting the melting temperature with the size of the cluster shows a non linear dependence on the size as can be noticed from Figure 11. This is expected since the properties of

the clusters depend directly on the ratio of surface to bulk atoms, which do not decrease linearly (section 3.2-3).

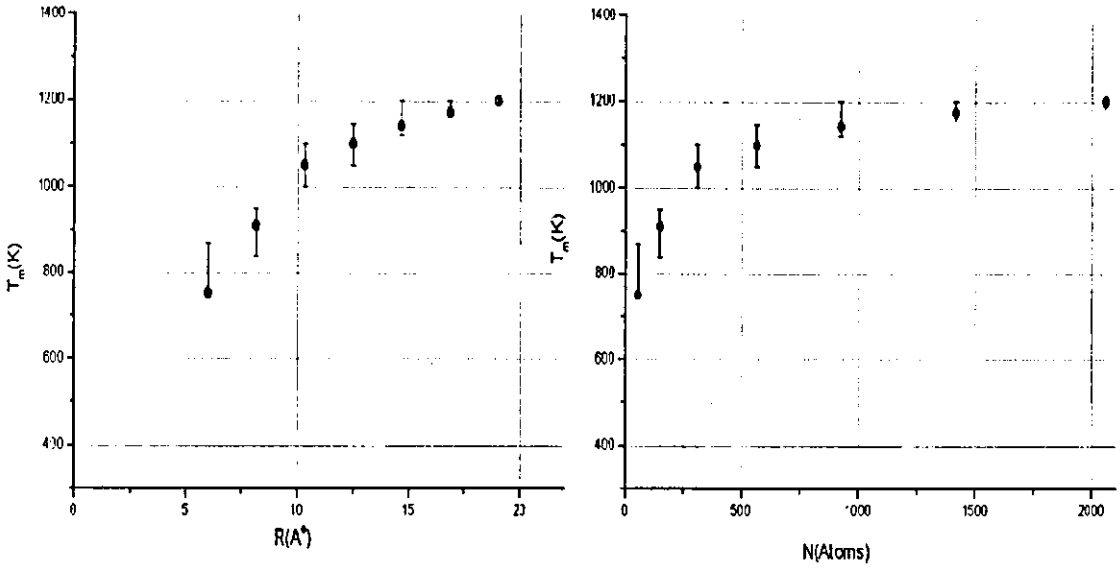

Figure 11 The melting temperature vs. the radius of the cluster R , and the number of atoms N

It is not only the melting temperature that depends on the cluster size; other cluster properties also depends on it. The latent energy of fusion per atom ΔE also increases with increasing the cluster size.

Since the atoms in smaller clusters are bonded to less atoms, and the ratio of surface to bulk atoms is large, where surface

atoms are less bonded than internal atoms, less heating is needed to get over the bonds so as melt the cluster. This is clear in the graph of the latent energy per atom ΔE against the radius of the cluster R, and against the number of atoms in the cluster N plotted in Figure 12.

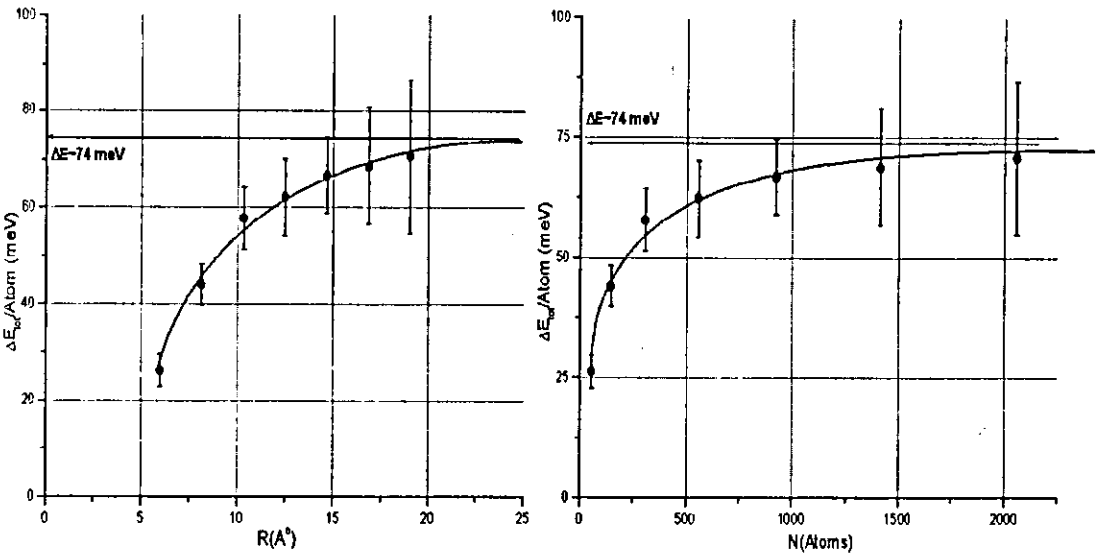

Figure 12 The latent energy of fusion (per atom) is plotted vs. N the number of atoms for the clusters, and the radius of the cluster R.

The main features of these figures are the asymptotic values which can be compared with the bulk simulation values and the error bars on the energy measurement to be related to the method used for the determination of the latent heat.

The error in the latent energy is substantial. The uncertainty was generated by combining the error in the y-intercepts of the two lines of E_{tot} per atom vs. the temperature.

As can be noticed for the clusters from Figures 11 and 12 where the melting temperatures and the latent energy per atom are plotted vs. the radius and the number of atoms in the cluster, respectively:

1. The melting temperature decreases with decreasing the size of the cluster.
2. The melting transition spreads over a region of melting temperatures. This region increases (became wider) with the decreasing size of the cluster.
3. The latent energy of fusion is also reduced with the decrease in the size of the cluster.
4. As the radius or the number of atoms in both figures goes to infinity, we can get the "simulated" values for the bulk.

These results agree with the done work on clusters in general: sodium, potassium, pair interacting atoms and some metallic clusters [28, 29,47,57-59].

A close look at the radial distribution function shows how it was affected by the melting. The sharp peaks start to disappear with time as one starts to approach the melting temperature.

We must notice that the peaks of large separation between atoms disappear earlier than those with smaller distances. This means that the direction of melting goes from the outermost shell to the inner shells as can be noticed from the radial distribution function as illustrated in Figure 13. This figure shows the radial distribution function (RDF) for the 2057 atoms palladium cluster along the melting process. At t=0 (Figure 13-a) the sharp peaks show a high degree of order; this is the initial cuboctahedral structure.

At temperatures near T_m, the changes to the radial distribution function shape and positions of the peaks occur after a few

picoseconds. This change is due to the transformation of the cluster from one structure (cuboctahedron) to another (icosahedron) Figure 13-b, plotted just before the transition, for the RDF after 25ps from the beginning of the simulation shows these changes: the peaks with large bins have disappeared due to the high temperature.

When the cluster begins melting, the direction of melting goes from outer shells towards the inner ones. The RDF for the melting of Pd_{2057} within 150ps (Figure 13-c) is plotted to show the structure at the beginning of the melting.

Figure 13-d shows the RDF at the end of the simulation (500ps), most of the peaks have disappeared, and the curve looks smooth.

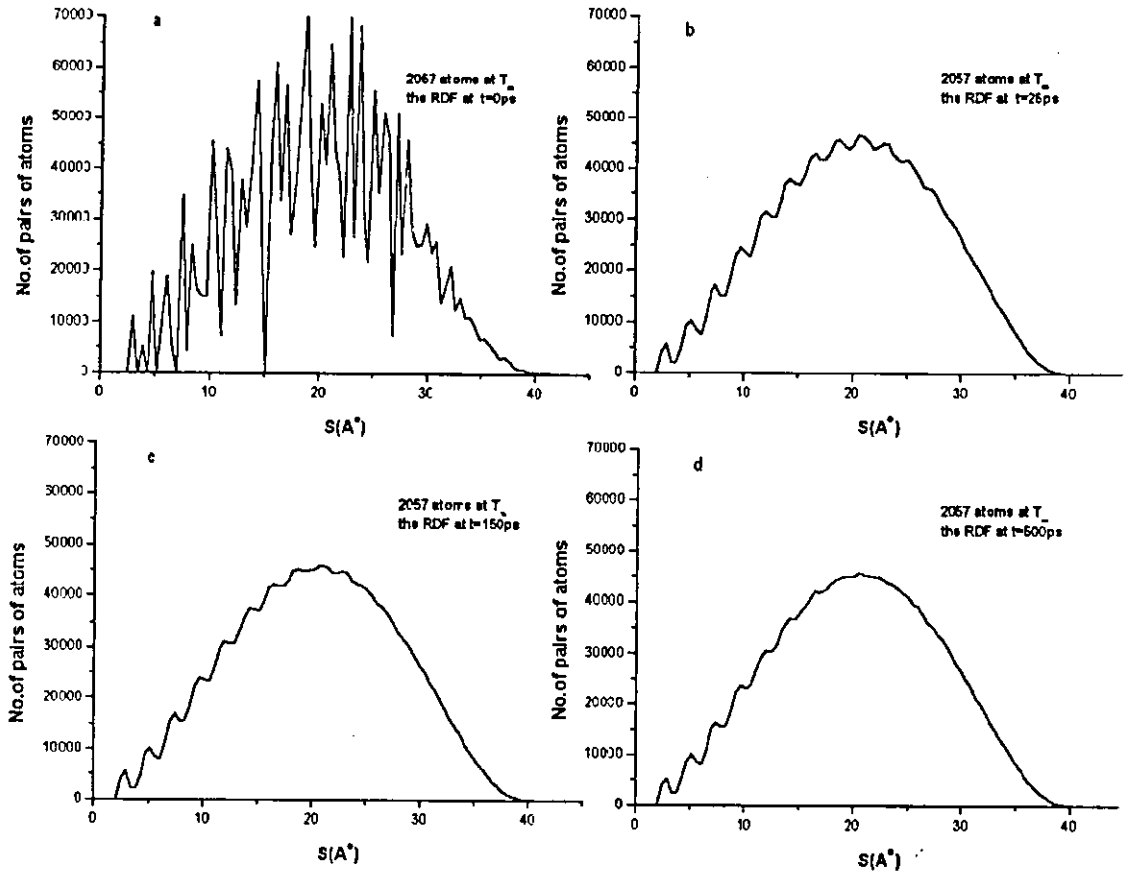

Figure 13 The radial distribution function for Pd_{2057} at T_m, the figures are taken before, during, and after the the melting process.

The discussion above leads to following synopsis of the steps of the melting process at T_m:

1. At the beginning of the simulation the atoms are in the initial positions in which they were prepared with the fcc cuboctahedral structure. The radial distribution function

RDF shows sharp peaks as expected from an ordered structure of pointlike atoms. This is illustrated in Figure 14(I) where we have drawn the RDF of the 561 magic cluster next to a 3-D image of the cluster.

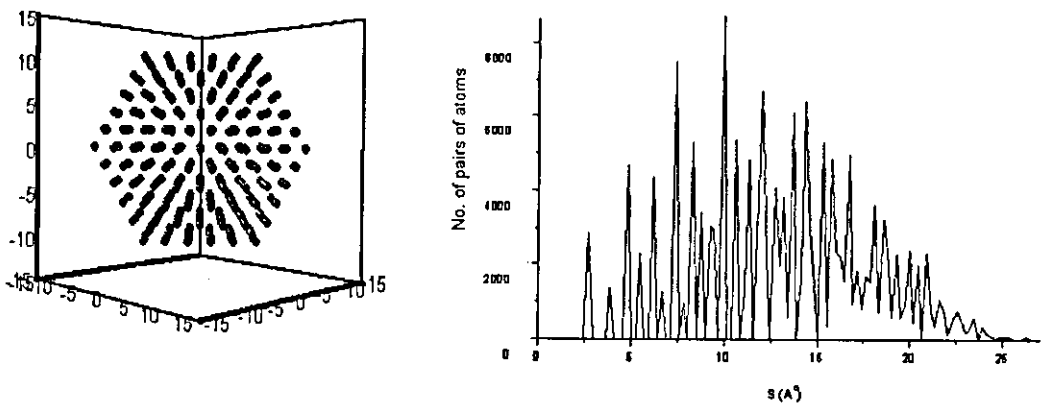

Figure 14(I) The shape and the RDF for Pd_{561} cluster at T_m as prepared

2. The cluster transforms with time from the cuboctahedral to the icosahedral structure which is a less energetic state. The resulting Icosahedron is not "a perfect" one because of the high temperatures. The RDF and the 3-D lattice image in Figure 14(II) show this conversion.

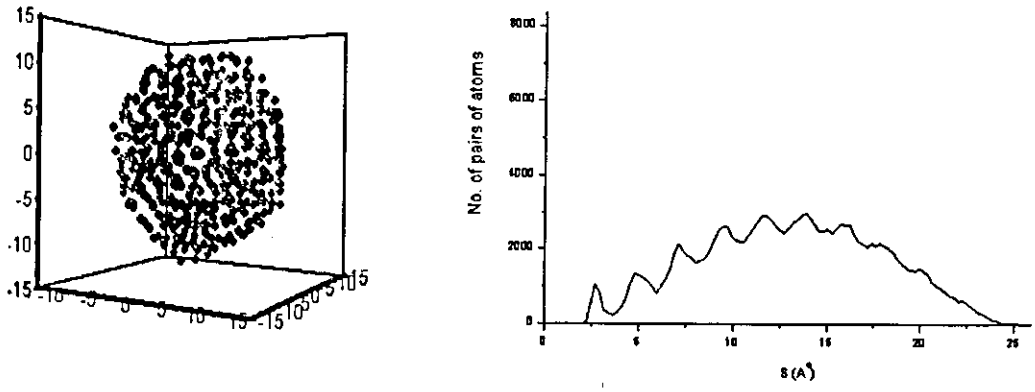

Figure 14(II) The shape and the RDF of the transformed Pd_{561} at T_m after 125ps [before melting]

3. The melting process starts after the conversion to the icosahedral structure. A jump in the energy appears clearly with a height equals ΔE the latent energy of fusion per atom, and the peaks of the RDF start disappearing with melting, in a direction from the outer shells to the inner shells.

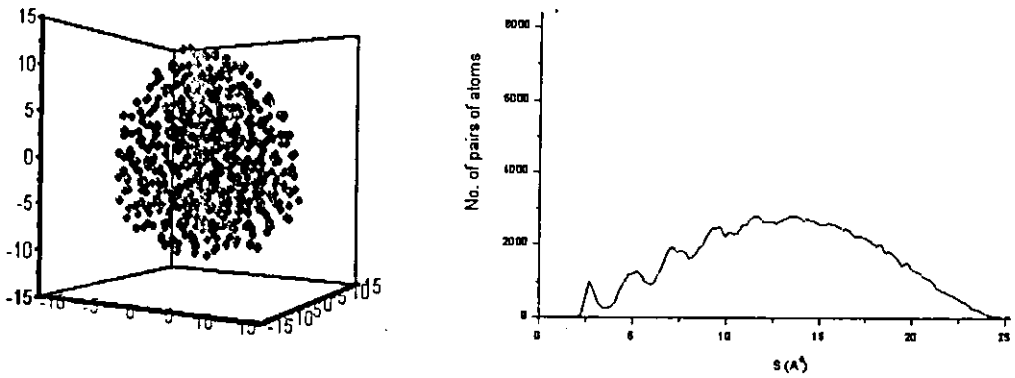

Figure 14(III) The shape and the RDF of the melted Pd_{561} at T_m after 375 ps [after melting]

The behavior depicted in Figures 14(I-III) for Pd_{561} is seen for all seven magic number clusters under investigation in this study.

The next figure is a summary of the whole simulation story of Pd_{561} at T_m. The progress is shown along the total energy-time curve for the cluster. The step of the latent energy per atom appears clearly.

An interesting result is the linear dependence of the melting temperature on cluster size. We see this by plotting the melting temperatures vs. $N^{-1/3}$ for the clusters simulated in this work. This is done in Figure 16 and as can be seen one gets an excellent linear fit.

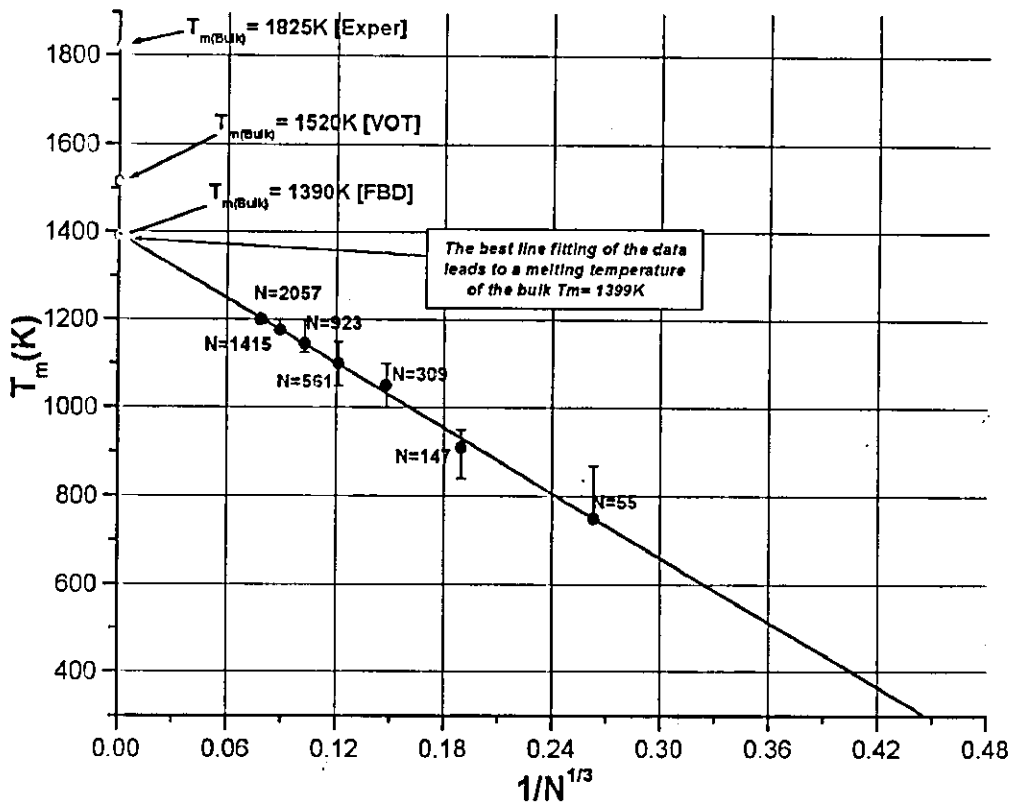

Figure 16 The linear relation between the melting temperature and $N^{-1/3}$ where N is the number of atoms in the cluster ,the figure shows the simulation T_m of the bulk when $N^{-1/3}$ goes to zero, T_m of the bulk for FDB[b], VOT[c] and experimental value are also shown

b Foiles and Adams, from reference [38]. c Ercolessi and Voter, of the same referenc

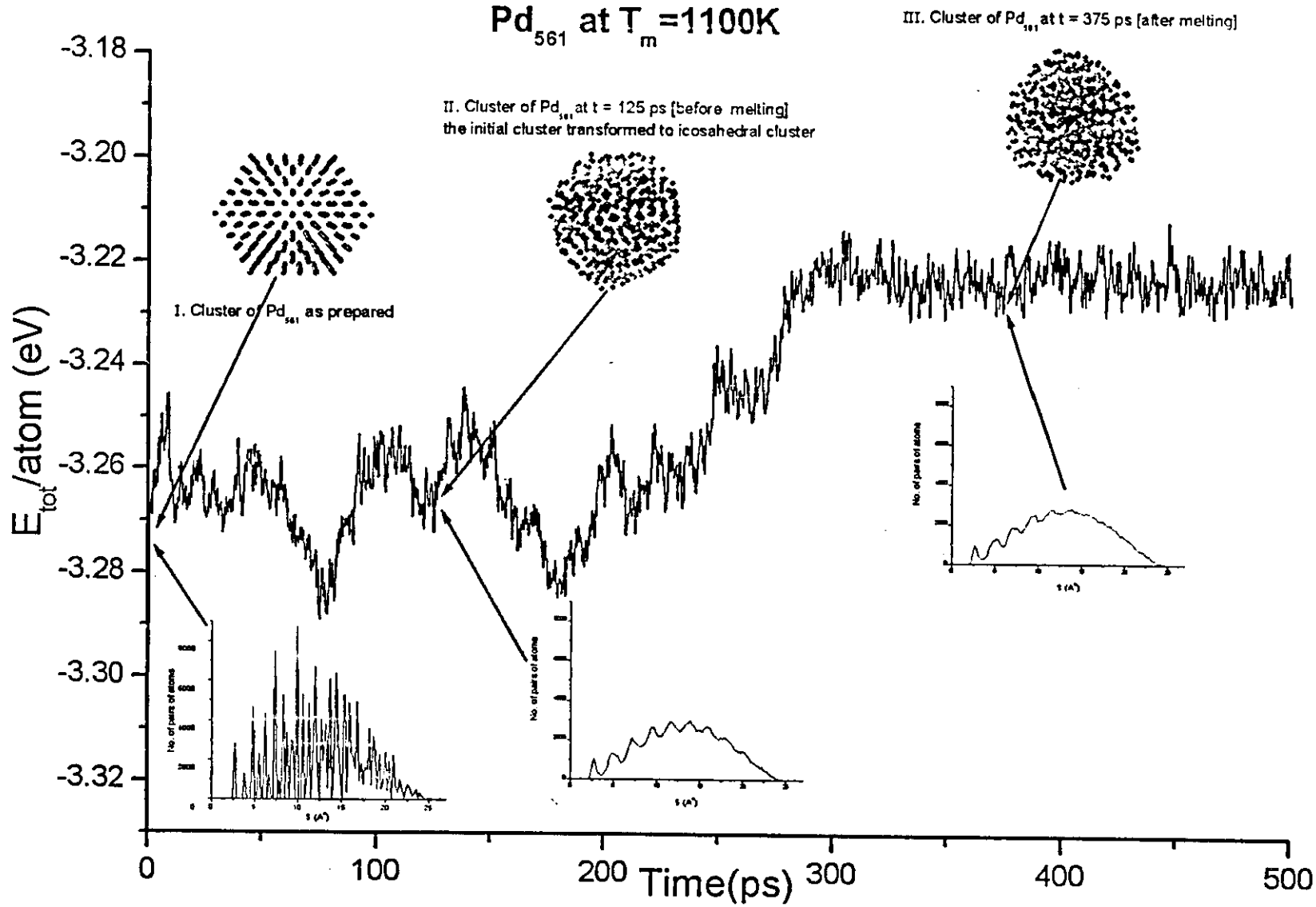

Figure 15 The total energy per atom vs. the time at T_m for Pd_{561}, the shape of the cluster and the radial distribution function are plotted as the simulation progresses

The y-intercept corresponding to $N = \infty$ which can be interpreted as the value for the simulated melting temperature for the bulk (where $N^{-1/3} \rightarrow 0$) of ~1400K.

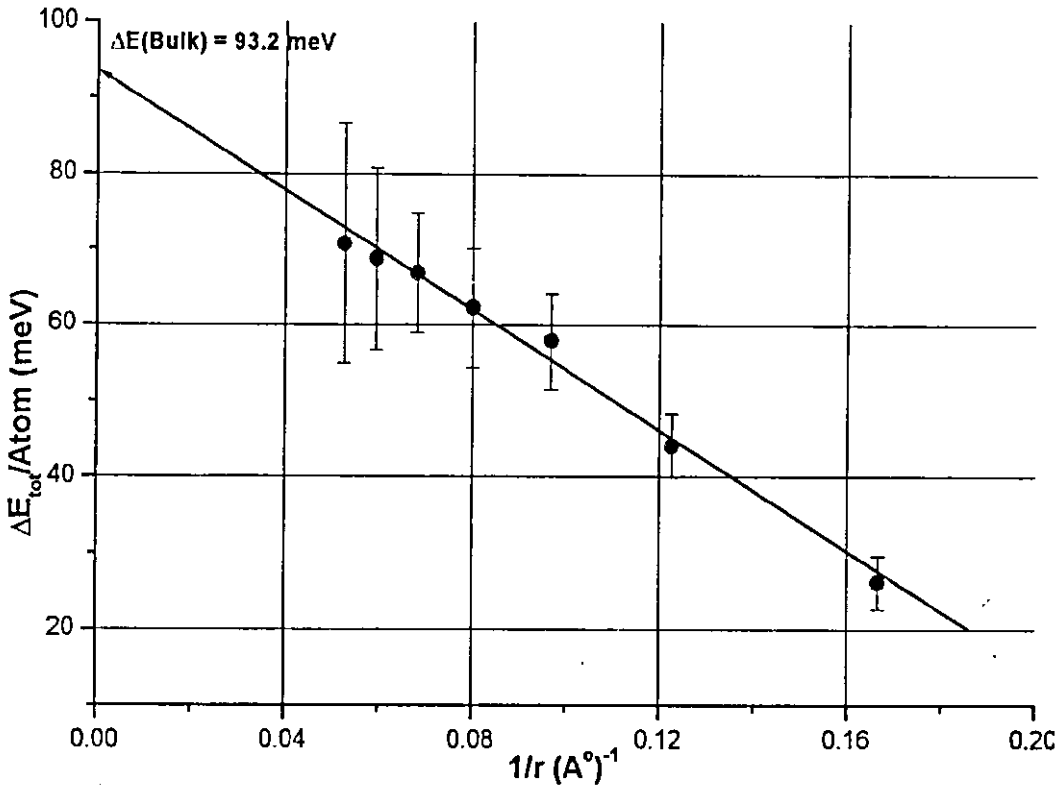

Figure 17 The latent energy per atom vs. 1/r gives the value of the latent energy of the bulk as 1/r goes to zero.

The same method could be used to determine ΔE more precisely. A plot of the latent energy per atom for the clusters ΔE vs. *1/r* where *r* is the radius of the cluster was made

(Figure17). It gives a value of ΔE for the bulk to be 93.2 meV, which is closer to the experimental value (table 3) than the asymptotic value determined in Figure 12.

Graphing the latent energy or the melting temperature gives the values for the bulk as r or N goes to infinity according to equations 30(a and b) of chapter 1. Using those equations, and the results of the best fitting to the data we can say that

$$\Delta E(r) = 93.2 - 396.1 r^{-1}$$

$$T_m(N) = 1399 - 2482.7 N^{-\frac{1}{3}}$$

Where r is in angstroms.

We must mention that at T=300K, three clusters transformed from cuboctahedral into Icosahedral structure, we took the average total energy per atom for those clusters in two regions, before and after the transformation.

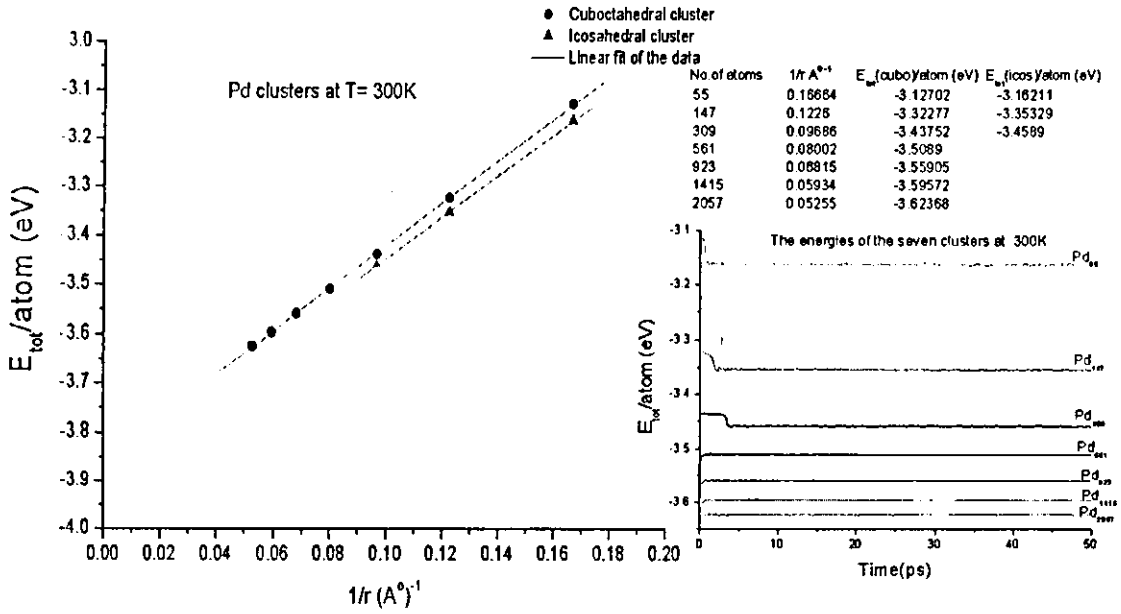

Figure 18 The total energy per atom as a function of 1/r, the result is two lines , the circles for the Cuboctahedral clusters, the triangles are for the transformed icosahedral structure. The figure to the right shows the energies at 300K for the seven clusters, where the step of the energy shows the transformation for the three smallest clusters.

At 300K, the three clusters that transforms at room temperature from cuboctahedral to icosahedral structure are: Pd_{55}, Pd_{147} and Pd_{309}. The energy of the three clusters changes because of the transformation, the energy of the cuboctahedral clusters is plotted in Figure 18 as circles, while the icosahedral cluster energy is plotted as triangles.

The variation of the average total energy per atom E_{tot}/atom as a function of cluster size at T=300K was plotted in Figure 19, it

has been found that E_{tot}/atom (including the interaction energy) in the cluster decreases and reaches an asymptotic value as cluster size increases.

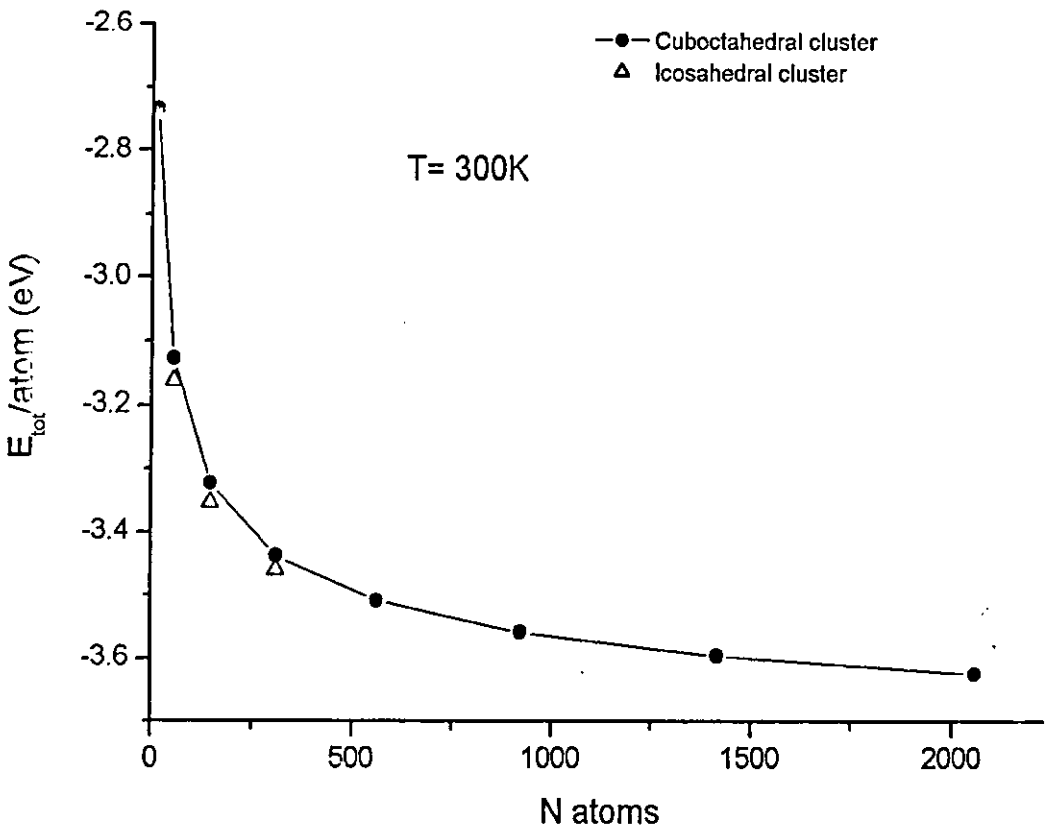

Figure 19 The total energy per atom as a function of the cluster size for untransformed Cuboctahedral clusters and the three converted Icosahedral cluster at T=300 K

Figure 19 contains these results with the connected energy data points for the clusters of cuboctahedral structure, while the triangles are for the energy of transformed clusters at 300K.

This looks as an exponential decay curve of the energy for the palladium clusters Pd_n (n= 13, 55, 147, 309, 561, 923, 1415, 2057) at T= 300K. Özdoğan and Erkoç [61] found the same curve for Copper clusters Cu_n (n=13, 19, 43, 55, 79, 135) at T=300K.

3.2.2 ICOSAHEDRON AND CUBOCTAHEDRON MELTING

At the melting temperature, the clusters of magic number of atoms that have initial icosahedral structure melt faster than those that have Cuboctahedral initial structure (with about 30ps in the case of Pd_{147}, Figure 20), because conversion to Icosahedron structure appears to be a precursor to melting.

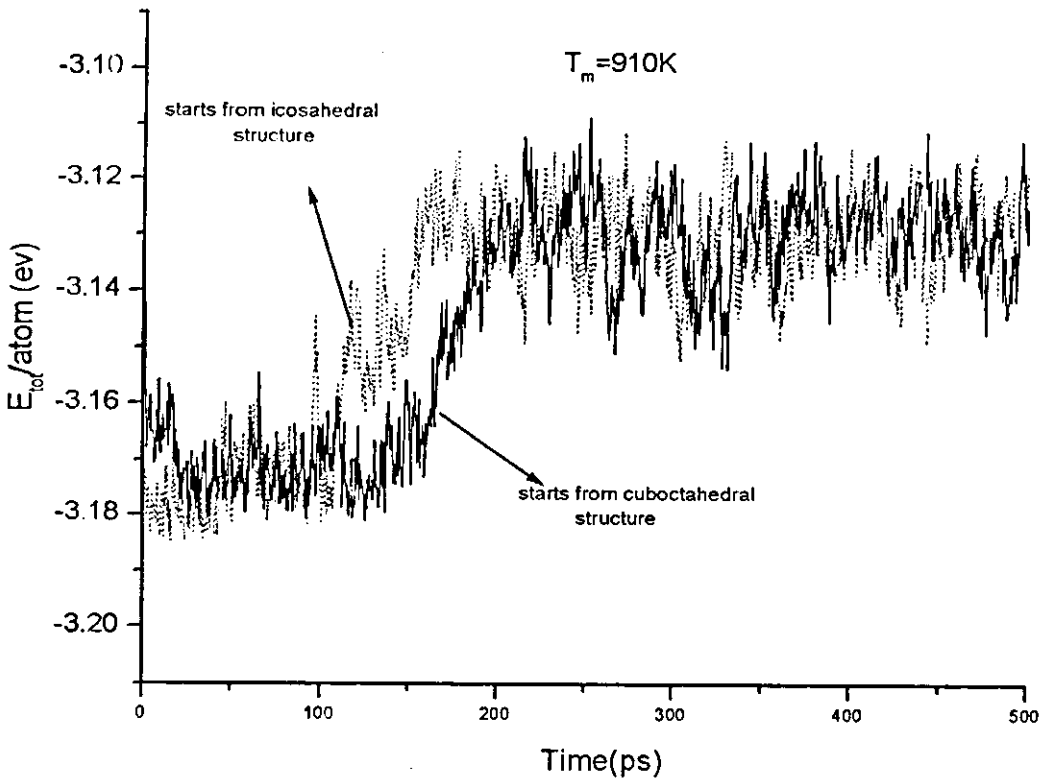

Figure 20 E_{tot}/Atom as a function of time for two palladium clusters of 147 atoms at T_m, the initial structures are Cuboctahedral for the first (Solid line) and Icosahedral for the second (Dotted line)

However, if one attempts to melt the cluster by placing near a reservoir above its melting temperature T_m, clusters of the cuboctahedral structure melt faster than icosahedral counterparts (For Pd_{147} the initially cuboctahedral structure starts melting with about 20ps earlier than the icosahedral cluster, Figure 21). They seem to melt directly from the

cuboctahedral structure without completing the conversion to the icosahedral structure. Icosahedral clusters treated the same way appear to be in need of longer times because they are more stable (since they are already an icosahedron).

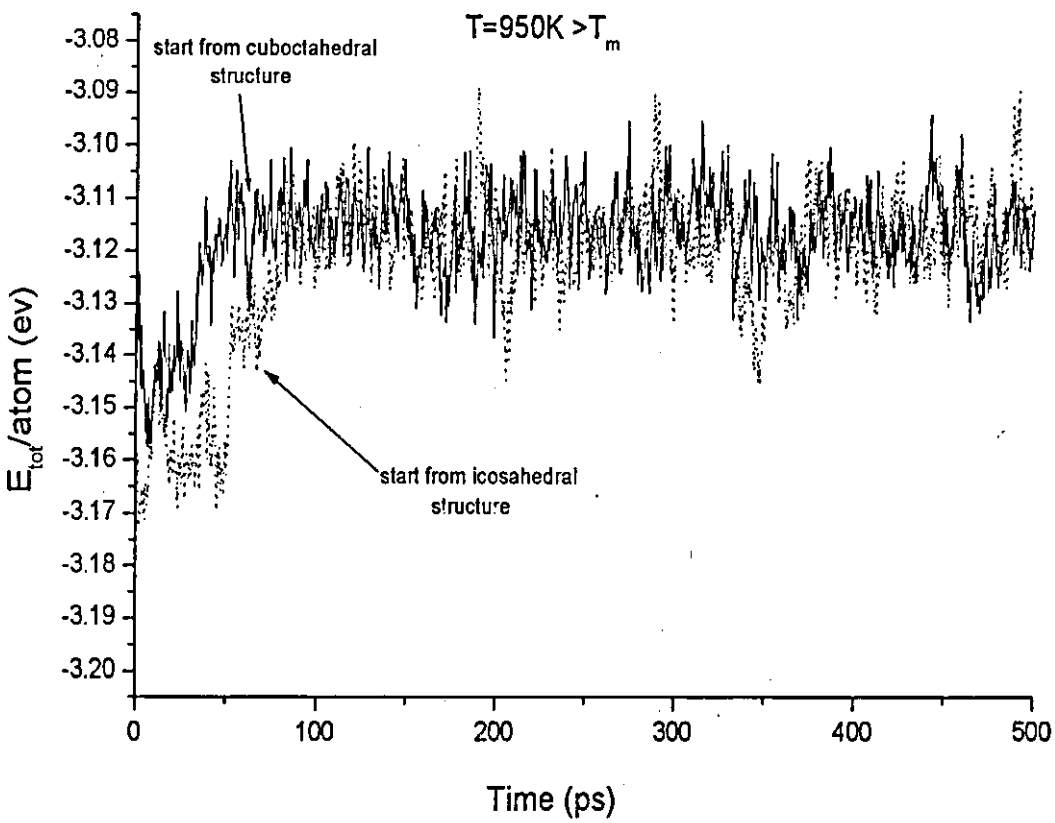

Figure 21 E_{tot}/Atom as a function of time for two palladium clusters of 147 atoms at T=950K (higher than T_m), the initial structures are Cuboctahedral for the first (Solid line) and Icosahedral for the second (Dotted line)

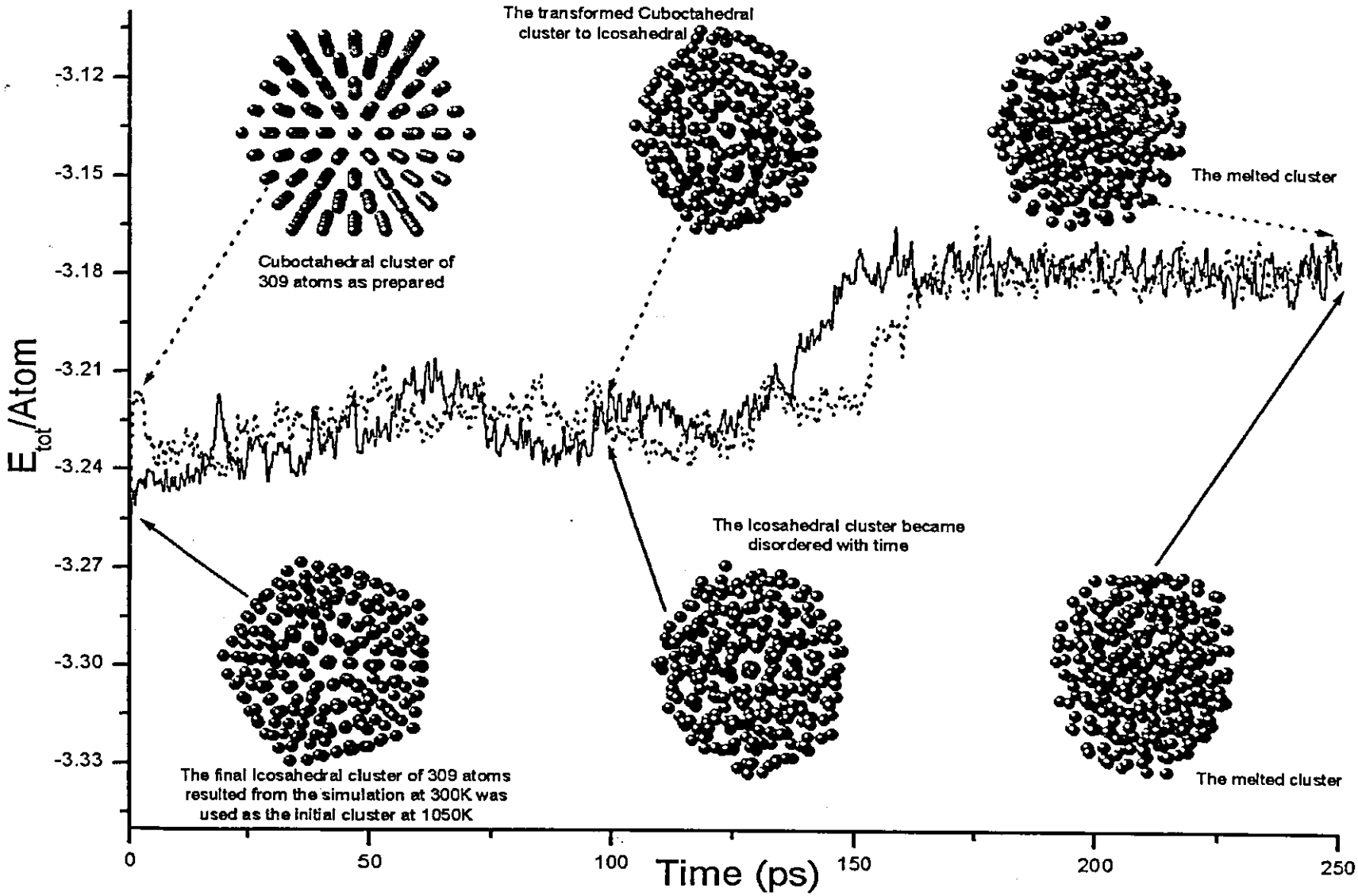

Figure 22 Total energy per atom as a function of time for two palladium clusters of 309 atoms at T_m of Pd_{309}= 1050K. The initial structures are cuboctahedral for the first (dotted line), and icosahedral for the second (solid line), where the progress of melting process is plotted with time. The shapes of the clusters are detected along the simulations of the two clusters.It's obvious that the cuboctahedral cluster converts to icosahedral cluster before melting, that's why it takes a loner time to melt at this temperature.

3.2.3 MELTING OF CLUSTERS WITH ATOMS OTHER THAN MAGIC NUMBERS.

Magic number clusters are more stable against melting than clusters with more or less atoms. Clusters with fewer or more atoms melt faster than their nearest magic numbers.

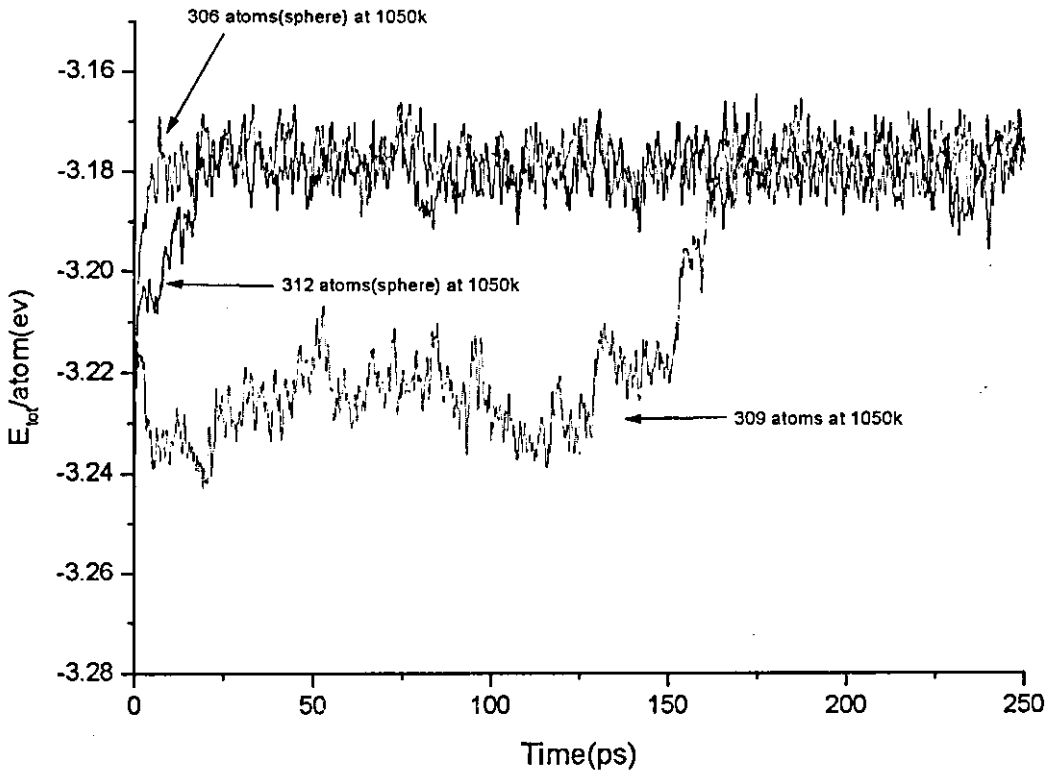

Figure 23 Three Pd clusters of 306,309,312 atoms in the fcc structure at 1050K, the cluster of the magic number 309 atoms is more stable (needs more time to melt)

This is illustrated in Figure 23 which shows the melting behaviors of two spheres were built, with different radii: the first with a radius of 2.646 Å contains 306 atoms, and the other with a radius 2.647Å contains 312 atoms. They were filled with palladium atoms that were distributed in the spheres in fcc-structure positions.

These clusters were melted at the same conditions of the icosahedral palladium cluster of 309 atoms, and at the same reservoir temperature. It was found that an fcc structure cluster of 306 or 312 atoms melts faster than that of icosahedral closed shells cluster with the nearest magic number, in this case one that contains 309 atoms.

The same was noticed when the cluster Pd_{2058} with fcc lattice structure that has a diameter d=4.97 nm. It melts faster than the icosahedral cluster of magic number 2057 atoms.

This is illustrated in Figure 24 where we can see that Pd_{2057} melts after ~180ps from beginning of the simulation while Pd_{2058} melts in less than 60ps.

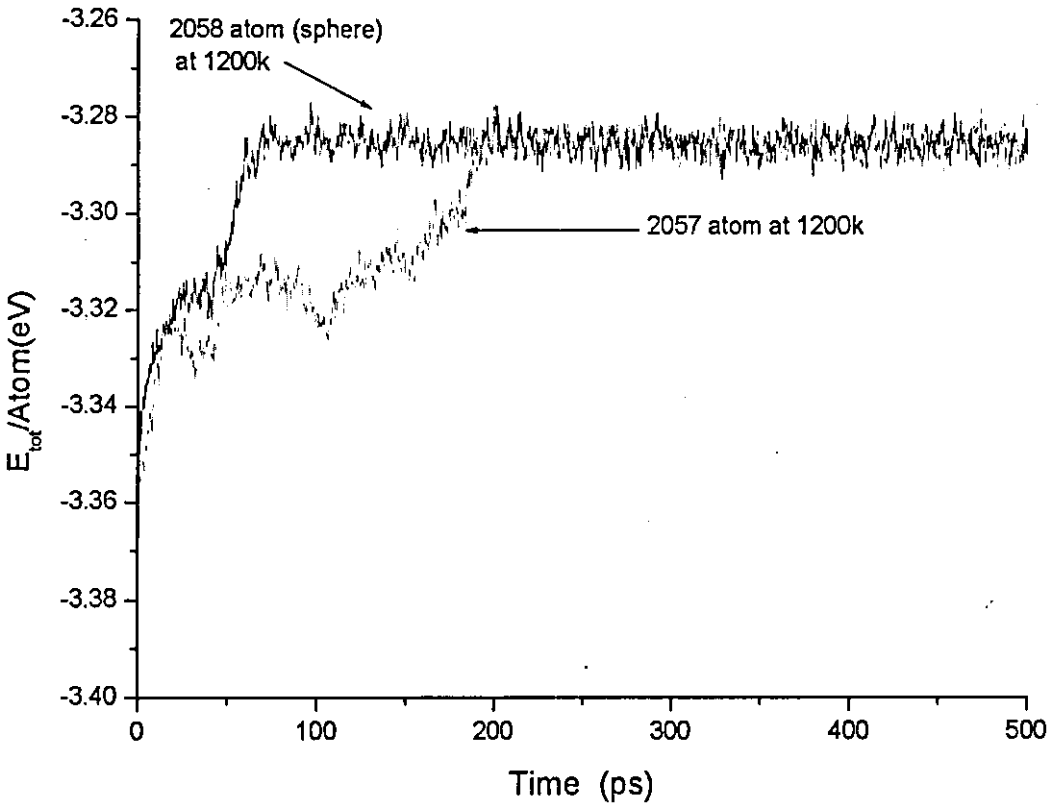

Figure 24 Two Pd clusters of 2057(green line), 2058 (blue line) atoms in the fcc structure at 1200K, the cluster of the magic number 2057 atoms is more stable.

3.2.4 COOLING OF CLUSTERS

It's known that if we start cooling a cluster, it will exhibit a hysterisis at the transition temperature [42]. To be sure that our

work is going in the right direction we did some simulations of cooling a cluster as a test to the hysterisis in the transition temperature.

We used the melted cluster of Pd_{147} that was produced at the end of the simulation at 910K. We quenched it to some temperatures that are several degrees below its melting temperature (from 880K to 860K). The resulting energy curves were averaged and added to the figure of E_{tot}/atom vs. temperature, the hysterisis was noticed clearly.

The transition during heating occurs at T=910K, while during cooling, it happened at T=870K (Figure 25). The low temperature of transition upon melting is a result of two things, the first is the limitation of MD time available for the cluster before melting (incomplete transition to the ground state), and the high temperature at which the cluster begins its transition at, which do not let atoms go to their icosahedral positions before meting (large facets are present).

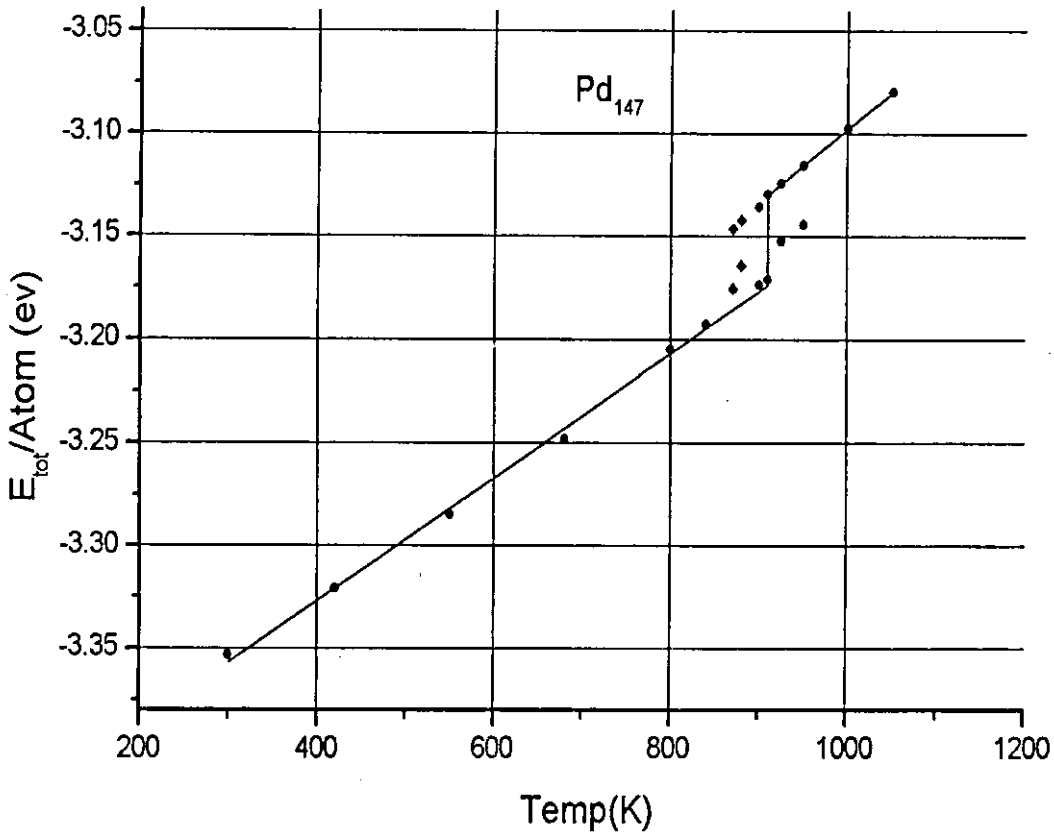

Figure 25 The melted Pd_{147} cluster was quenched, the hysterisis in the transition temperature is noticed ($T_{heating}$ =910K, $T_{cooling}$ =870K)

3.2.5 THE MELTING CHARACTERISTICS OF VERY SMALL CLUSTERS

For very small clusters T_m decreases as the cluster size increase [52, 56, 57, 61] seems that very small clusters have markedly different properties from those of larger ones.

Smaller clusters have a very high melting temperature this was noticed for clusters with less than 50 atoms. We demonstrated this fact by simulating the melting of Pd_{13}.

Figure 26 shows the total energy per atom, plotted against time, at T=1000K, and T=1200K. The energy curves show a fluctuation between completely solid and completely melted material, so that we can say that the cluster really melts at those temperatures. While at 1500K and 2000K the cluster is melted even if its energy is highly vibrating, the melting is clear within the first ~3 picoseconds of the energy curve.

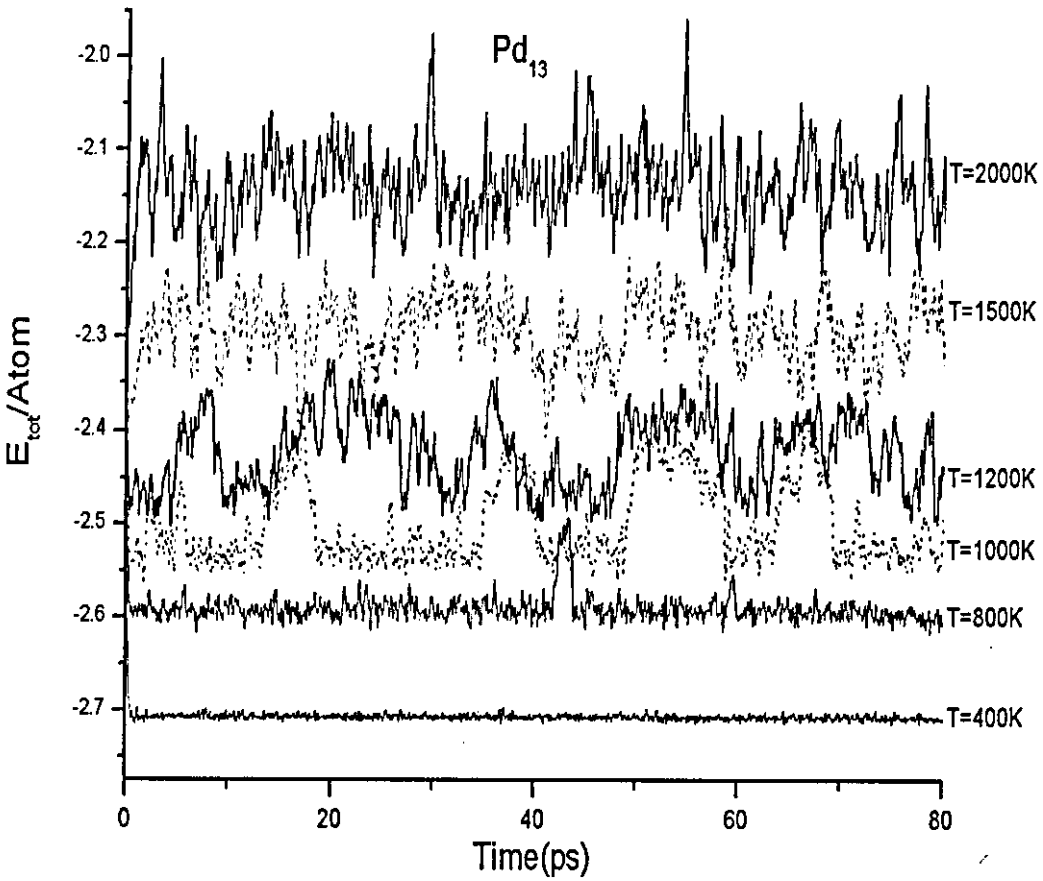

Figure 26 E_{tot}/Atom as a function of time at different temperatures shows the high melting temperature for Pd_{13}

As was mentioned in table 4; the melting temperatures of Pd_{55} is750K and for Pd_{2057} it is1200K. The melting temperature of Pd_{13} is very high.

3.3 A DETAILED ANALYSIS OF ONE OF THE CLUSTERS

In this section, we describe in enough details, the results of simulating the behavior of the magic number cluster Pd_{309}. Pd_{309} is made of 5 shells. Simulations were done at the temperatures, 300K, 500K, 700K, 850K, 900K, 1000K, 1050K, 1065K, 1085K, 1100K, 1150K, 1200K, 1400K, 1750K and 2000K.

As the simulations started for the Pd_{309} cluster; the cuboctahedral cluster converted into icosahedral cluster, of closed shells. The icosahedral Pd_{309} cluster, has the index $k=5$ of four shells surrounding the central atom.

The transformation at low temperature appears clearly. The icosahedral structure is lower in energy. In figure 27, the transformation of Pd_{309} at 300K is shown, with the shape of the cluster and the radial distribution function.

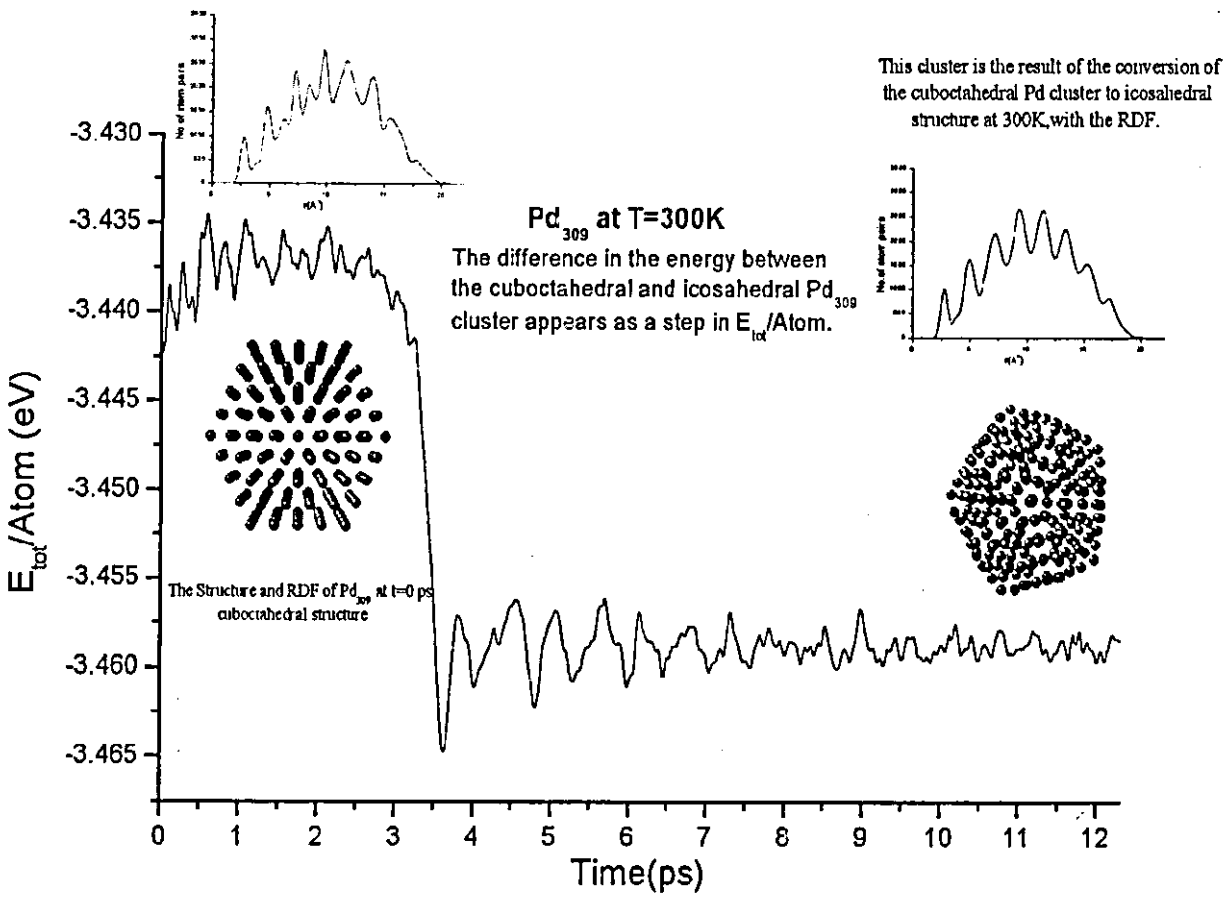

Figure 27 E_{tot}/atom with time shows the change in the energy caused by the transformation of the cuboctahedral cluster to icosahedral cluster.

The transformation of the Cuboctahedral cluster to icosahedral cluster was noticed for all the simulations done at temperatures less or included in the melting region. While at higher

temperatures, the melting occurs before the transformation takes place.

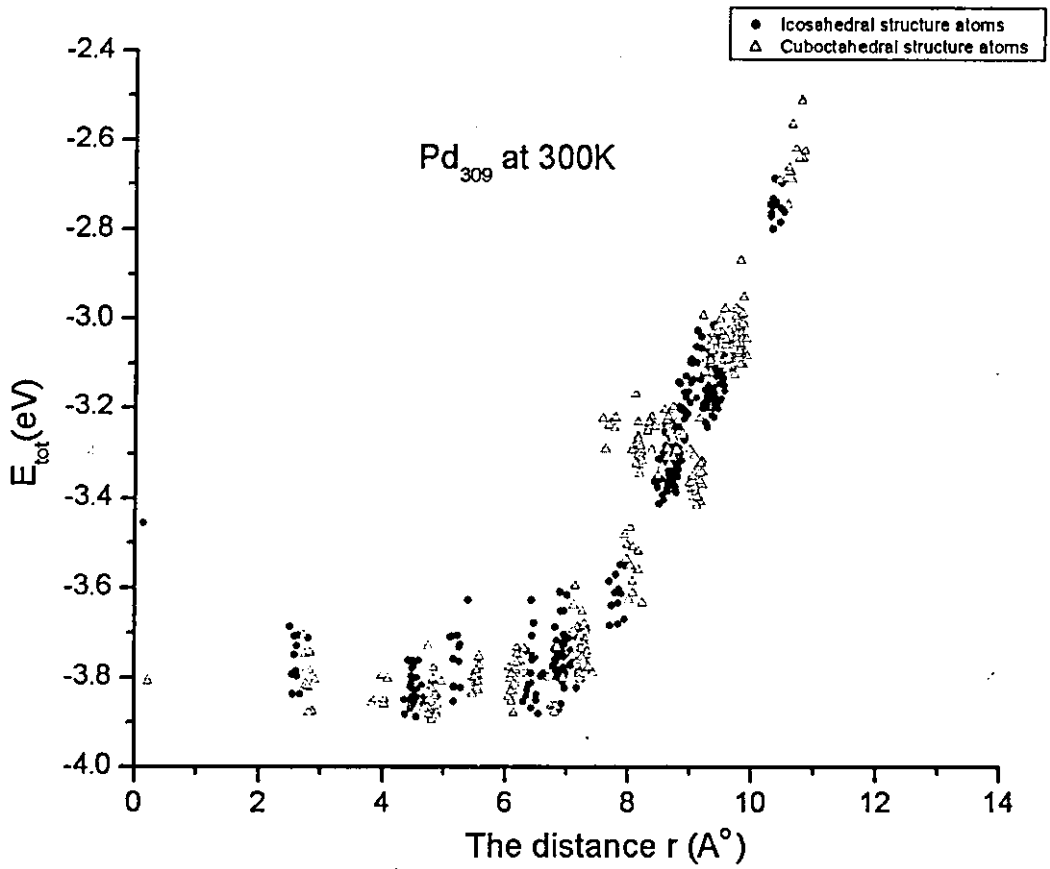

Figure 28 The total energy for each atom of the Cuboctahedral structure and the icosahedral structure atoms as a function of the radial position of each atom.

The difference in energy caused by the transformation of the cluster can be noticed on the energy of individual atoms. Figure 28 shows the total energy plotted against the radial distance of

the atoms to the centre of the cluster. For each atom in both the initial cuboctahedral and transformed icosahedral cluster, reflects that difference; the energies of the outer shell atoms are lower for the icosahedral cluster (Figure 28).

Melting was clearly noticed at T=1050K according to the changes in the total energy per atom with time (Figure 29).

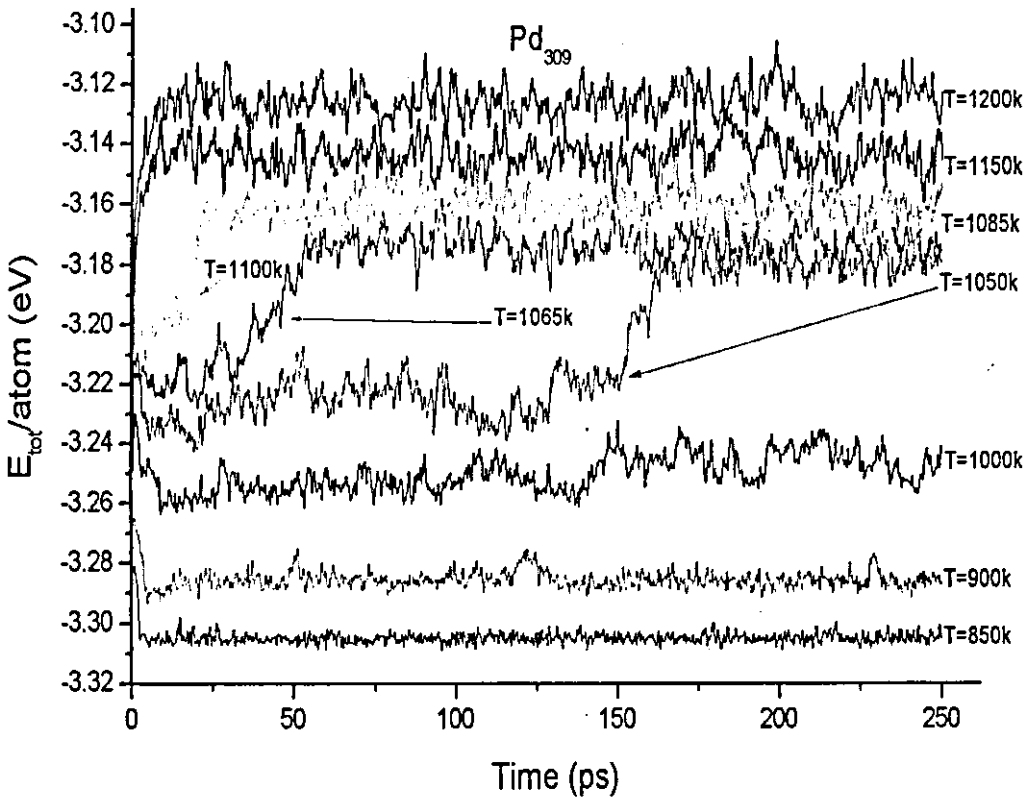

Figure 29 The total energy per atom vs. time for Pd_{309}cluster at nine different temperatures, the melting is observed clearly at 1050K

At 1065K, 1085K, 1100K the melting occurs but it is faster than the time we suggested (the melting happens within 5-50ps, while we usually consider the time of melting between 100ps and 400ps) so these temperatures were included in the uncertainty of the melting temperature T_m=1050K , at which the melting happens in the period between 140ps to 170ps.

ΔE was calculated for Pd_{309} from the graph of the average total energy per atom with temperature to be ~58meV at the melting temperature T_m which is 1050K from the same figure (Figure30).

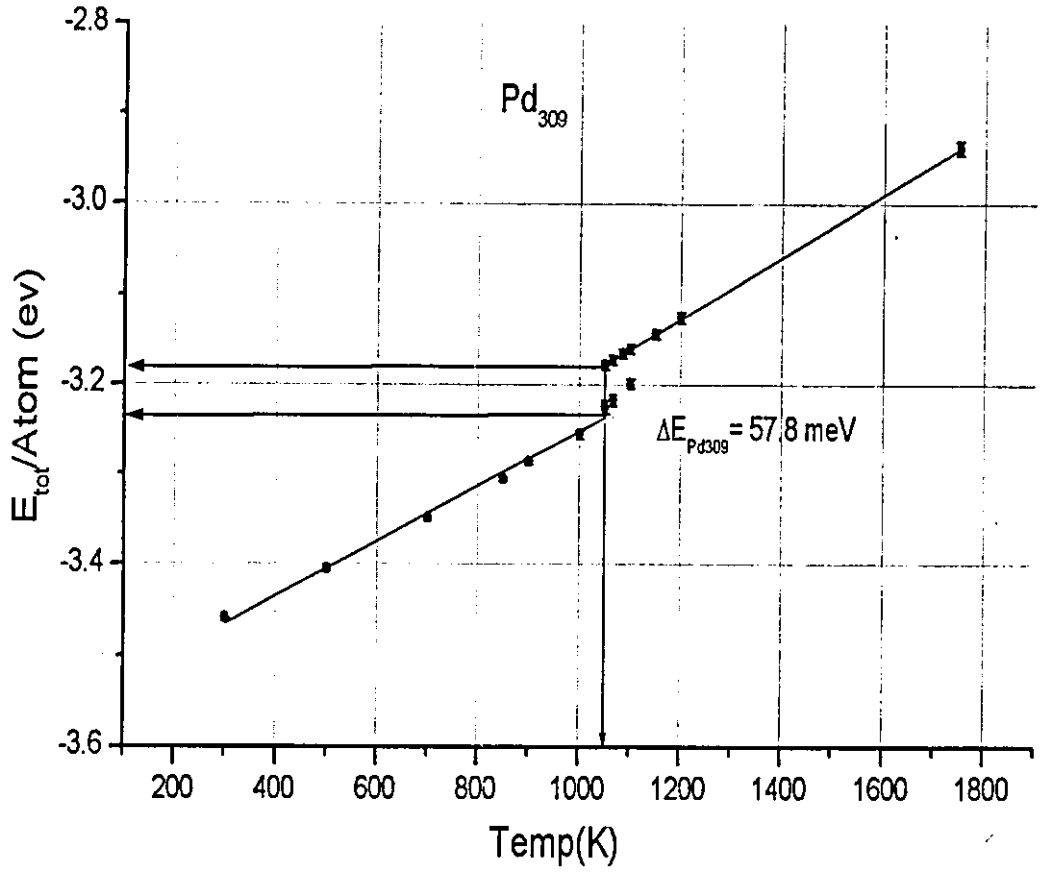

Figure 30 The total energy per atom vs. Temperature for the Pd_{309} cluster, melting is observed clearly at 1050K, and the latent energy ΔE is calculated to be about 58 meV

Figure 31 Pd_{309} shows the "total energy per atom" vs. time at T_m, the period of time (0-15 ps) is marked to show the Cuboctahedron – Icosahedron transition which occurs after about 6 ps of the beginning of the simulation at T_m .

The pictures and the radial distribution functions are shown along the melting simulation to show the transformation and the melting details.

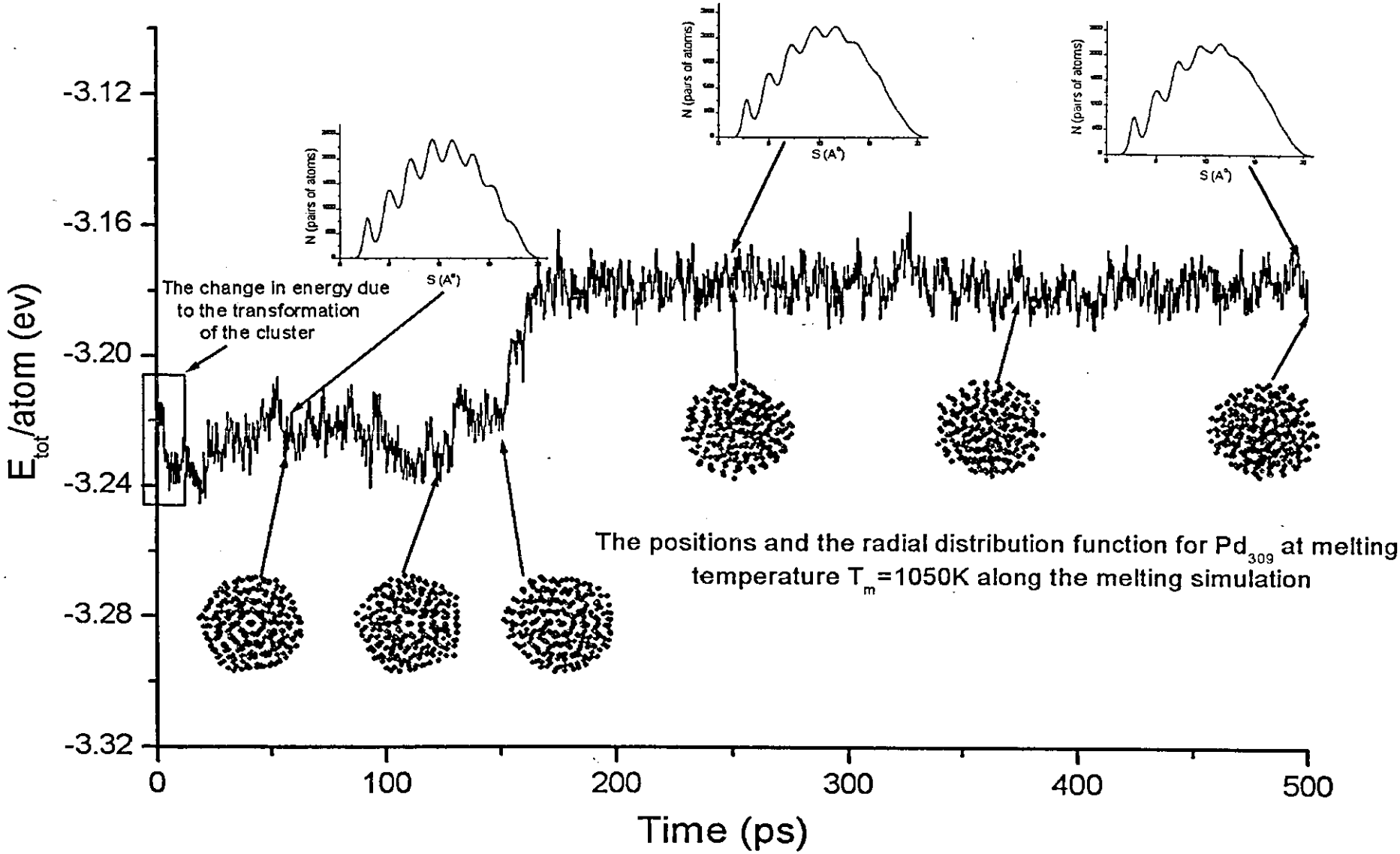

Figure 31 A detailed figure of Pd_{309} at melting temperature shows clearly the transformation of the Cuboctahedral cluster to icosahedral cluster in about 6 ps then the melting process starts after about 150ps, with the shape and the RDF of the clusters.

SUMMARY AND CONCLUSION

The subject of this thesis is the study of the melting dynamics of Nanoscale palladium clusters; the embedded atom method potential was employed using the molecular dynamics simulation.

In chapter one, several important "background" subjects were discussed: The history of particle simulation was briefly studied. The Molecular Dynamics Simulation techniques, mathematics, and statistical mechanics were covered. An overview of the interatomic potentials, with a detailed study of the embedded atom method was done.

The Atomic clusters, especially those with magic numbers of atoms; their structures, melting temperatures, and metallic behaviors where also discussed.

In chapter two the technical part was done: Building of the Cuboctahedral clusters using the **latgen** code was discussed.

An overview of the molecular dynamics simulation software, with a detailed description of the simulation software XMD was also done.

In chapter three, the data was analyzed to get the main results of this thesis. Our main results can be summarized in a few main points:

1. The melting temperatures of the clusters are lower than that of the bulk. They increase with increasing the size of the cluster.
2. The latent energy of fusion increase when increasing the cluster size.
3. Cuboctahedral palladium clusters of magic numbers of atoms at melting temperatures convert to icosahedral clusters before melting.
4. The clusters of magic numbers of atoms are more stable since they need longer time to melt than clusters of other numbers of atoms (at the same temperature).

5. The Icosahedron of magic number of atoms is also more stable than the Cuboctahedron of magic numbers of atoms.
6. A hysterisis of the transition temperature was noticed when cooling the melted cluster.
7. A very high temperature of melting for the very small clusters, this was investigated for the Pd_{13} which have a very high melting temperature.

Finally; the thesis results are generally consistent with results for other metallic clusters work results. Some melting properties of the palladium clusters of magic number were clarified in this work.

APPENDICES

APPENDIX I

*Table 5: Some software for molecular dynamics simulation**

SOFTWARE	DESCRIPTION	LINK
AMBER	MD &energy minimization program	http://www.amber.ucsf edu/amber/
AMMP	MM&MD and modeling program, C	http://www.cs.gsu.edu/~cscrwh/ammp/ammp.html
AW3	(ARTwork) MD&MC simulation program, based on effective medium theory.	http://www.aue.auc.dk/~stoltze/artwork/aw3/features.html
CAMELION	3-D MD&MC program, fortran77 Suitable using EAM&MEAM, parallelized version fortran90	http://www.tm.tudelft.nl/secties/fcm/matphy/software/software.htm
CHARMM	MC,MD &energy minimization program	http://www.ch.embnet.org/MD_tutorial/ http://yuri.harvard.edu/ http://www.ch.embnet.org/MD_tutorial/pages/index2.html
DL_POLY	A parallel MD simulation package	http://igen.ch.kcl.ac.uk/ccwp/dl_poly_orig.html http://www.dl.ac.uk/TCSC/Software/DL_POLY/main.html
DYNAMO	MD simulation library, using MM & hybrid MM/QM potentials using Fortran 90	http://www.ibs.fr/ext/labos/LDM/projet6/welcome_en.htm
EGO	A parallel & Sequential MD simulation program, computes molecular trajectories.	http://www.lrz-muenchen.de/~heller/ego/
FHI98md	Perform density functional theory total-energy calculations for materials ranging from insulators to transition metals	http://www.fhi-berlin.mpg.de/th/fhi98md/
Ghemical	MM,MD software package, C++, under the GNU GPL	http://www.uku.fi/~thassine/ghemical
GROMACS	Complete Versatile MD & energy minimization package	http://www.gromacs.org/
GROMOS	A general purpose MD simulation package	http://www.igc.ethz.ch/gromos/
GULP	Simulation of 3D solids, Gas phase clusters ,.....molecular solids and ionic materials, fortran77 and fortran90	http://www.ccwp.ac.uk/ccwp/gulp.html http://www.ch.ic.ac.uk/gale/Research/gulp.html

LAMMPS	A parallel MD simulation program for molecular and atomic systems	http://www.cs.sandia.gov/~sjplimp/lammps.html http://www.wag.caltech.edu/home-pages/mario/lammps2001/README.html
MDRANGE(MDH)	MD program for the simulation of high energy particles	http://beam.helsinki.fi/~knordlun/mdh/mdh_program.html
MDynaMix	A parallel MD simulation package for the simulation of mixtures, Fortran77	http://www.fos.su.se/physical/sasha/md_prog.html
Mindy	Simple MD program derived from NAMD,C++.	http://www.ks.uiuc.edu/Development/MDTools/mindy/
MMTK	Molecular Modeling Toolkit , for molecular simulations	http://starship.python.net/crew/hinsen/MMTK/
Moldy	A general purpose MD simulation program for molecular, ionic and atomic systems, C	http://www.earth.ox.ac.uk/~keith/moldy.html http://citeseer.nj.nec.com/refson98moldy.html
MOSCITO	MD program for the simulation of rigid and/or flexible molecules, for PC's & Supercomputers"	http://ganter.chemie.uni-dortmund.de/~pas/moscito.html
NAMD	Parallel object-oriented MD simulation program	http://biowulf.nih.gov/namd-ug/ http://www.ks.uiuc.edu/Research/namd/
NEMD	Nonequilibrium MD program (Macintosh)	http://rsc.anu.edu.au/RSC/NEMD.html http://www.anu.edu.au/Physics/summerschool/NEMD/Welcome.html
PARADYN	Parallel MD program using EAM potential (based on serial DYNAMO code) using Fortran 90 and C	http://www.cs.wisc.edu/paradyn/ http://www.cs.sandia.gov/~sjplimp/main.html
SIgMA	System of programs for MD & energy minimization	http://femto.med.unc.edu/SIGMA/
SOLVATE	MD simulation for atomic macromolecule model	http://www.mpibpc.gwdg.de/abteilungen/071/solvate/docu.html
Tinker	A complete general MM,MD software package	http://dasher.wustl.edu/tinker/
VASP	*Ab-initio* Quantum MD simulation package	http://tph.tuwien.ac.at/~vasp/
XMD	Performs MD (CMD) simulations on metals and ceramics	http://www.ims.uconn.edu/centers/simul/#xmd

SOME MD SOFTWARE FROM THE CCP5 PROGRAM LIBRARY	http://www.dl.ac.uk/CCP/CCP5/librar.html
ADMIXT	MD simulation of atomic mixtures. Short range Lennard-Jones atom-atom forces. Verlet leapfrog algorithm.
HMDIAT3	MD program for diatomic molecules using the quaternion algorithm.
HSTOCH	MD program, stochastic dynamics, constraint algorithm
MCMOLDYN	MC& MD simulation package for water systems
MD3DLJ	MD for Lennard-Jones atoms in 3 – dimensions , pc/workstation C- language program

MDATOM	MD simulation program for Lennard-Jones atoms, using predictor corrector algorithm
MDDIAT	Program for MD simulation of diatomics
MDIONS	Program for MD simulation of ionic systems using the Ewald summation
MDLIN	MD simulation program for linear molecules using the quaternion algorithm
MDMANY	Program for MD simulation of rigid non-linear polyatomicS
MDMEGA.F	Program for MD simulation of Lennard-Jones atoms with a spherical cutoff
MDMIXT	Program for MD simulation of molecular mixtures. With short range Lennard-Jones site-site forces
MDMPOL	Program for MD simulation of rigid polyatomic molecules
MDMULP	Program for MD simulation of rigid polyatomic molecules with short range Lennard-Jones site-site forces combined with electrostatic point multipole long range forces
MDNACL	MD simulation of alkali halide systems
MDPOLY	MD simulation program for rigid polyatomic molecules using the quaternion algorithm.
MDSGWP	Program for MD simulation of Gaussian wave packets
MDTETRA	MD simulation program for tetrahedral molecules using the quaternion algorithm.
MDZOID	Program for MD simulation of Gaussian molecules
SOTON_PAR	Program for MD simulation of Lennard-Jones atoms using link- cells MD algorithm

*This table was done in may 2002; the information was collected from the internet and organized here.

APPENDIX II

Latgen progrom for generation of Cuboctahedral lattices

```
#include <iostream.h>
#include <fstream.h>
#include <math.h>

int atom,kp,kh,k,ntypes=2,tot,n,shells=5,nhyd=0,hndx=0,pndx=0;
float ax[5],ay[5],az[5],f,init_tim=0.;
float gx,gy,gz,i,boltz=8.617e-5;
float Pdx[1000],Pdy[1000],Pdz[1000];
float Hdx[1000],Hdy[1000],Hdz[1000];
float alat=3.89;
float vel1,vel2,vel3;
float amass[2]={0.1044688350000000E-03,0.1102836000000000E-01};
int iclement[2]={1,46};
float perub[3]={0.9725000000000000E+01,0.9725000000000000E+01,0.9725000000000000E+01};
float perlb[3]={-0.9725000000000000E+01,-0.9725000000000000E+01,-0.9725000000000000E+01};
double laenge_in_111,projektion;

void main()
{
 ifstream infile;
 ofstream outfile;
 ofstream printer;
 char filename[20];
outfile.open("new.dat");

      tot = 0;
      for(k=1;k<=shells;k++)
            { tot = tot + 10*k*k+2; }
            tot = tot+1; /* Add central atom */

            outfile <<nhyd <<"\t"<<tot<<"\n";
            outfile <<amass[0] <<"\t"<<amass[1] <<"\n";
            outfile << init_tim <<"\n";
            outfile << 2*perub[0] <<"\t"<< 2*perub[1]<<"\t"<< -2*perub[2]<<"\n";

i=5;
f=1;
laenge_in_111=(double)i/sqrt(3.);
for (gx=-8.; gx<=8.; gx++)
  {
    for (gy=-8.; gy<=8.; gy++)
      {
        for (gz=-8.;gz<=8.;gz++)
          {
            ax[1]=(float)gx;
            ay[1]=(float)gy;
            az[1]=(float)gz;
            ax[2]=(float)(gx+0.5);
            ay[2]=(float)gy;
            az[2]=(float)(gz+0.5);
            ax[3]=(float)(gx+0.5);
            ay[3]=(float)(gy+0.5);
```

```
          az[3]=(float)gz;
          ax[4]=(float)gx;
          ay[4]=(float)(gy+0.5);
          az[4]=(float)(gz+0.5);
          for (atom=1; atom<=4; atom++)
          {
           projektion=(double)(sqrt(1./3.)*(fabs(ax[atom])+fabs(ay[atom])+fabs(az[atom])));
           if
((projektion<=laenge_in_111)&&(fabs(ax[atom])<=i/2.)&&(fabs(ay[atom])<=i/2.)&&(fabs(az[atom])<=i/2.
))
           {
           pndx=pndx+1;
           Pdx[pndx]=alat*ax[atom];
           Pdy[pndx]=alat*ay[atom];
           Pdz[pndx]=alat*az[atom];
           hndx=hndx+1;
           Hdx[hndx]=ax[2];
           Hdy[hndx]=ay[3];
           Hdz[hndx]=az[4];

          }
          }
        }
      }
  }
     for(kh=1; kh<nhyd ;kh++)
     for(kp=1; kp<pndx ;kp++)
          {
          outfile << Pdx[kp] <<"\t"<< Pdy[kp] <<"\t"<< Pdz[kp]<<"\n";
          }
     for(kh=1; kh<nhyd ;kh++)
     for(kp=1; kp<pndx ;kp++)
          {
//          outfile << vel1 <<"\t"<< vel2 <<"\t"<< vel3 <<"\n";
          }
//          outfile << 0. <<"\t"<< 0. <<"\t"<< 0. <<"\n";

}
```

REFERENCES

1. Vashishta P., Bachlechner M.E., Campbell T., Kalia R.K., Kikuchi H., Kodiyalam S., Nakano A., and Walsh P., (2001) Computing Laboratory for Materials Simulations, Department of Physics & Astronomy and Department of Computer Science, Louisiana State University. Retrieved 17 March 2002. http://www.cclms.lsu.edu/cclms/teaching/csc7610/00Intro.pdf and references

2. Stote R., (October 1999) Theory of molecular dynamics simulations and references Retrieved August 2002 from the CHARMM molecular dynamics simulation web site. http://www.ch.embnet.org/MD_tutorial/pages/MD.Part1.html

3. Alder B.J., and Wainwright T.E., (1957) , J. Chem. Phys, **27**, 1208.

4. Alder B.J., and Wainwright T.E., (1959). J. Chem. Phys, **31**, 459.

5. Marshall V.,(October 1997), First-principles molecular dynamics, Retrieved 18 August 2002 , http://www.dl.ac.uk/TCS/MatSci/Projects/Techniques/fpmd.html

6. Rahman A., (1964). Phys.Rev. A, **136**, 405.

7. Stillinger F. H., and Rahman A., (1974). J. Chem. Phys, **60**, 1545.

8. Finnis M., Atomistic simulation group, School of Mathematics, The Queen's university, Belfast, UK (2001), Interatomic forces in materials ,The Hume-Rothery Memorial Lecture 2001, held at the department of materials, university of Oxford in (23 October 2001), ...(and references)

9. Car R., and Parrinello M., (1985), Unified Approach for Molecular Dynamics and Density- Functional Theory. Phys.Rev.Lett. 55, 2471-2474.

10. Daw M.S., and Baskes M.I., (1984).Embedded-atom method: Derivation and application to impurities, surfaces and other defects in metals. Phys.Rev.B, 29, 6643-6453

11. Foiles S.M., Baskes M.I., and Daw M.S., (1986). Embedded-atom functions for the fcc metals Cu, Ag, Au, Ni, Pd, Pt, and their alloys. Phys.Rev.B, **33**, 7983-7991

12. Takahashi K., EAM series and their history. Retrieved 25 October 2001 Tokyo Institute of Technology http://www.mcp.titech.ac.jp/Ktakahashi/

13. Zhigilei L.V., (Spring 2002) Modeling in Materials Science (MSE 524), Retrieved 28 June 2002. University of Virginia, Department of Materials Science and Engineering http://www.people.virginia.edu/~lz2n/mse524/

14. Smith B., Molecular simulation group. Molecular Simulation Retrieved 17 March 2002. Computational Science and Engineering department. Daresbury Laboratory http://www.cse.dl.ac.uk/LinearActivity/179

15. Côté A.S., Smith B., Lindan P.J.D., (2001), Retrieved 20 August 2002, Daresbury Laboratory http://www.compsoc.man.ac.uk/~lucky/Democritus/Theory/moldyn1.html

16. Ercolessi F., (June 1997) A molecular dynamics primer, (Spring collage in Computational Physics, ICTP, Trieste, June 1997)

17. Côté A.S., Smith B., Lindan P.J.D. (2001), Retrieved 20 August 2002, Daresbury Laboratory http://www.compsoc.man.ac.uk/~lucky/Democritus.

18. Zhigilei L.V., (Spring 2002) Modeling in Materials Science (MSE 524), Retrieved 28 June 2002, University of Virginia, Department of Materials Science and Engineering http://www.people.virginia.edu/~lz2n/mse524/notes-2002/Pressure.pdf

19. Bekker H.,(1996) Molecular Dynamics Simulation Methods Revised, Retrieved 9 August 2002 . http://www.ub.rug.nl/eldoc/dis/science/h.bekker/thesis.pdf

20. Biosym/MSI ,Release 95.0/3.00 (October 1995), Molecular Dynamics-Pressure and Stress, Retrieved 20 August 2002. Copyright Biosym/MSI Response Center. San Diego http://gagliano.phys.s.utokyo.ac.jp:8000/members/jkura/discover/General/Dynamics/Press_Stress.html#Contr

21. Briels W.J., (October 1998) Theory of Polymer Dynamics, the radial distribution function, Retrieved 21 August 2002 http://tnweb.tn.utwente.nl/cdr/PolymeerDictaat/node14.html

22. Côté A.S., Smith B., Lindan P.J.D. (2001), Radial distribution function, Retrieved 8/20/2002, Daresbury Laboratory http://www.compsoc.man.ac.uk/~lucky/Democritus/Theory/rdf.html http://www.compsoc.man.ac.uk/~lucky/Democritus/Theory/disfun.html http://www.compsoc.man.ac.uk/~lucky/Democritus/Experiments/exp4.html

23. Gotwals B., (1999) overview of the Born-Oppenheimer Approximation Retrieved 7 April 2002, ChimViz development team http://www.shodor.org/chemviz/overview/boa.html

24. Sherrill C.D., (January 1996) The Born-Oppenheimer Approximation Retrieved 7 April 2002, http://www.adi.uam.es/Docs/Knowledge/Fundamental_Theory/quantrev/node28.html

25. Boston University Center for Polymer Studies, Wasser program, Molecular Model for Water, Retrieved 13 August 2002 http://polymer.bu.edu/Wasser/robert/work/node8.html.

26. Kittle C., (1996) Introduction to Solid State Physics, (7th ed.). Canada, Wiley & Sons, page 60

27. Sun D.Y., Gong X.G., (1996), Molecular- Dynamics study on the equilibrium structure and stability of a cluster dimmer, Phys.Rev.B ,54,17051.

28. Smirnov B.M., (1994), Melting of clusters with pair interaction of atoms, Physics-Uspekhi 37(11)1079-1097.

29. Lee Y.J., Nieminen R.M., Lee E., Kim S., (2001) universal melting behaviour of clusters, Computer Physics Communications , **142**, 201-205

30. Celestini F., Pellenq R.J.M., Bordarier P., and Rousseau B., (1996), Melting of Lennard-Jones Clusters in confined geometries, Z.Phys. D., **37**, 49-53.

31. Wales D.J., Doye J.P.K., Dullweber A., Hodges M.P., Naumkin F.Y., Calvo F., Hernández-Rojas J., and Middleton T.F., The Cambridge Cluster Database, Retrieved 18 August 2002, http://www-wales.ch.cam.ac.uk/CCD.html.

32. Tersoff J., (1989) Modeling solid-state chemistry: Interatomic potential for multicomponent systems. Phys.Rev.B 39, 5566.

33. Kittle C., (1996) Introduction to Solid State Physics, (7th ed.). Canada, Wiley & Sons, page 73

34. Ercolessi F., Parrinello M., Tosatti E., (1988) Philos. mag. A, 58 (1), 213.

35. Finnis M. W., and Sinclair J.E., (1984), Philos. mag. A, 50(1), 45-55.

36. Jacobson K.W., Nørskov J.K., and Puska M.J., (1987). Interatomic interaction in the effective-medium theory. Phys.Rev.B. 35, 7423-7442.

37. Baskes M.I., (1992) Modified embedded-atom potential for cubic materials and impurities. Phys.Rev.B . 46, 2727-2742.

38. Wolf R.J., Mansour K.A., Lee M.W., and Ray J.R., (1992), Temperature dependence of elastic constants of embedded-atom models of palladium, Phys.Rev.B 46, 8027-8035 and references.

39. Soulé de Bas B.J., (May 2001). Simulation of Bulk and Grain Boundary Diffusion in B2 NiAl , Master's thesis. Virginia Polytechnic Institute and State University ,Blacksburg, Virginia

40. Pundt A., Domhiem M., Guerdane M., Ehrenberg H., Reetz M.T., and Jisrawi N.M., (2002) Evidence for cubic-to-icosahedral transition of quasi-free Pd-H-clusters controlled by the hydrogen content. Eur. Phys. J. D 19, 333-337.

41. Jisrawi N.M., Critical size for the cuboctahedral to icosahedral structure phase transition in nanometer-sized Pd clusters (unpublished) .

42. Lewis L.J., Jensen P., and Barrat J.L., (1997), Melting, freezing and coalescence of gold nanoclusters ,Phys.Rev.B 56, 2248,.

43. Nam H.S., Hwang N.M., Yu B.D., and Yoon J.K., (21 August 2002) Formation of an Icosahedral Structure during the Freezing of Gold Nanoclusters: Surface-Induced Mechanism, Retrieved 24 August 2002 http://xxx.lanl.gov/PS_cache/physics/pdf/0205/0205024.pdf

44. Bilalbegovic' G., (1998). Structure and stability of finite gold nanowires. Phys.Rev.B, 58, 15412.

45. Kröger M., (2000), Metal foams via embedded atoms simulation retrieved 27 August 2002 http://www.mat.ethz.ch/dwerk/oettinger/MK_DIR/pmk51/paper.pdf

46. De Heer W.A., (1993), The physics of simple metal clusters: experimental aspects and simple models Rev.Mod.Phys., 65,611-676.

47. Martin T.P., (1996) Shells of Atoms. Phys. Rep. 273, 199-241.

48. Hofmeister H., (1998) Forty Years Study of Fivefold Twinned Structures in Small Particles and Thin Films Cryst. Res. Technol. 33 , 1, 3-25

49. Mackay A.L., (1962). Acta Cryst. 15, 916.

50. Johnston R. L.,(1998). The development of metallic behaviour in clusters, Phil. Trans. R. Soc. Lond. A . 356, 211–230,. .....and references

51. DiTolla F., Ercolessi F., Tartaglino U., Santoro G., and Tosatti E., (2000) Surface Physics SISSA Group . Retrieved 14 August 2002, http://www.sissa.it/cm/sp

52. Shvartsburg A.A., Jarrold M.F., (2000), Solid Clusters above the Bulk Melting point. Phys.Rev.Lett. 85, 2530.

53. Lai S.L., Guo J.Y., Petrova V., Ramanath G., and Allen L.H., (1996), Size-Dependent Melting Properties of Small Tin Particles: Nanocalorimetric Measurements. Phys.Rev.Lett. 77, 99.

54. Qi Y., Cagin T., Johnson W.L., GoddardIII W.A., (2000) Size Dependence of Melting and Crystallization in Ni Nanoclusters, Retrieved 18 August 2002, http://www.wag.caltech.edu/anmeeting/2000/presentations/yqi/

55. Lee Y.J., Lee E., Kim S., and Nieminen R.M., (2001) Effect of potential energy distribution on the melting of clusters. Phys.Rev.lett. 86, 999.

56. American Physical Society. (December 2000). Retrieved 24 August 2002 http://focus.aps.org/v6/st11.html

57. Kusche R., Hippler Th., Schmidt M., von Issendorf B., and Haberland H., (1999), Melting of free sodium clusters, Eur. Phys. J. D. 9, 1-4.

58. Schmidt M., Kusche R., Hippler Th. Donges J., Kronmüller W., von Issendorf B., and Haberland H., (2001),Negative Heat Capacity for a Cluster of 147 Sodium Atoms Phys.Rev.Lett. 86, 1191.

59. Aguado A., Molina L.M., Lopez J.M., and Alonso J.A., (2001) Melting behavior of large disordered sodium clusters, Eur. Phys. J. D. 15,221-227.

60. Aguado A., (2001). An orbital free molecular dynamics study of melting in K20, K55, K92, K142, Rb55 and Cs55 clusters. Phys.Rev.B. 63,115404

61. Özdoğan C., Erkoç Ş., (1997) Molecular-dynamics simulation of structural stability, energetics, and melting of Cu_n (n=13-135) clusters Z.Phys. D 41, 205-209.

62. Nielsen O.H., (1994). Melting a copper Cluster: Critical droplet theory. Europhysics Lett. 26,51.

63. Nielsen O.H., Sethna J.P., Stoltze P., Jacobsen K.W., and N_rskov J.K., (1994) Melting a Copper Cluster, Negative Specific Heat. Laboratory of Applied Physics, Technical University of Denmark. Retrieved 18 August 2002. http://www.lassp.cornell.edu/sethna/CrystalShapes/CopperCluster.html

64. Rifkin J., XMD-Molecular Dynamics Program, jrifkin@mail.ims.uconn.edu v2.5.22 (19 Jan 1999)

65. Lee S.H., Lee S.C., Lee K.R., Lee K.H. and Lee J.G.,(2002)Meta-stable Sites in Amorphous Carbon Lattice Generated by Rapid Quenching of Liquid Diamond. Korea Institute of Science and Technology, P. O. Box 131, Cheongryang, Seoul, Korea, Retrieved 25 August 2002 http://diamond.kist.re.kr/DLC/publication/pdf/cp-27.doc

66. Clapp P., Rifkin J., Fernando G., (March 2000). Center for Materials Simulation, University of Connecticut Institute of Materials Science *jon.rifkin@uconn.edu* http://www.ims.uconn.edu/centers/simul/xmd/doc-2.5.30/xmd-12.html#ss12.4

67. Clapp P., Rifkin J., Fernando G., (March 2000). Center for Materials Simulation, University of Connecticut Institute of Materials Science *jon.rifkin@uconn.edu* http://www.ims.uconn.edu/centers/simul/pot/potformat.htm

68. Grönbeck H., Tomànek D., Kim S.G., and Rosén A., (1997), Hydrogen induced melting of Palladium clusters, Z.Phys.D 40,469–471

69. Kaszkur Z., (2000), Nanopowder diffraction analysis beyond the Bragg law applied to palladium J. Appl. Cryst., 33, 87.

70. Kaszkur Z., (2000), Powder diffraction beyond the Bragg law: study of palladium nanocrystals J. Appl. Cryst., 33, 1262.

ديناميكيات الانصهار لعناقيد البلاديوم
باستخدام نظرية جهد الذرة المطمورة.

THE MELTING DYNAMICS OF NANOSCALE Pd CLUSTERS
(A Molecular Dynamics Study Using the Modified Embedded Atom Method)

موضوع هذه الأطروحة يتناول دراسة ديناميكية الانصهار المتعلقة بعناقيد ذرات البلاديوم (Palladium clusters) باستخدام أسلوب المحاكاة للقوى الجزيئية أو المحاكاة لديناميكيات الجزيئات (Molecular Dynamics Simulation) التي توظف جهد الذرة المطمورة أو المدفونة بشكل خاص(Embedded atom potential)[1,2].

تم أولا بحث تاريخ تطور المحاكاة الجزيئية (Molecular simulation) بشكل مقتضب من حيث التقنيات و التفصيلات الإحصائية و الرياضية، و غطى البحث معظم أنواع الجهود الداخلية المتعلقة بالذرات(Interatomic Potentials) خاصة جهد الذرة المطمورة.

---

[1] Daw M.S., and Baskes M.I., (1984).Embedded-atom method: Derivation and application to impurities, surfaces and other defects in metals. Phys.Rev.B, 29, 6643-6453

[2] Foiles S.M., Baskes M.I., and Daw M.S., (1986). Embedded-atom functions for the fcc metals Cu, Ag, Au, Ni, Pd, Pt, and their alloys. Phys.Rev.B, 33, 7983-7991

كما تم نقاش موضوع العناقيد بشكل عام و العناقيد المتعلقة بعنصر البلاديوم ذات السطوح المغلقة أو المحكمة (Closed Shells) بشكل خاص و التي تسمى بعناقيد البلاديوم ذات الأعداد السحرية(Magic Number Palladium Clusters)[4,3].

و بتحليل مستفيض لنتاج البيانات التي استخلصت باستخدام المحاكاة الجزيئية لعناقيد البلاديوم أثناء الانصهار تم التوصل إلى عدة نتائج تتلخص فيما يلي:

1. درجة حرارة الانصهار للعناقيد (The Clusters) هي أقل من تلك الخاصة بالكتل (The Bulk) وترتفع بازدياد حجم العنقود.
2. تزداد الطاقة الكامنة للانصهار(Latent Energy of Fusion) أيضا بازدياد حجم العنقود.
3. العناقيد المحكمة السطوح من ذرات البلاديوم ذات البناء (Cuboctahedron) و التي لها أعداد سحرية تتحول إلى البناء (Icosahedron) محكمة السطوح قبل بدء عملية الانصهار.

---

[3] Martin T.P., (1996) Shells of Atoms. Phys. Rep. 273, 199-241.

[4] Mackay A.L., (1962). Acta Cryst. 15, 916.

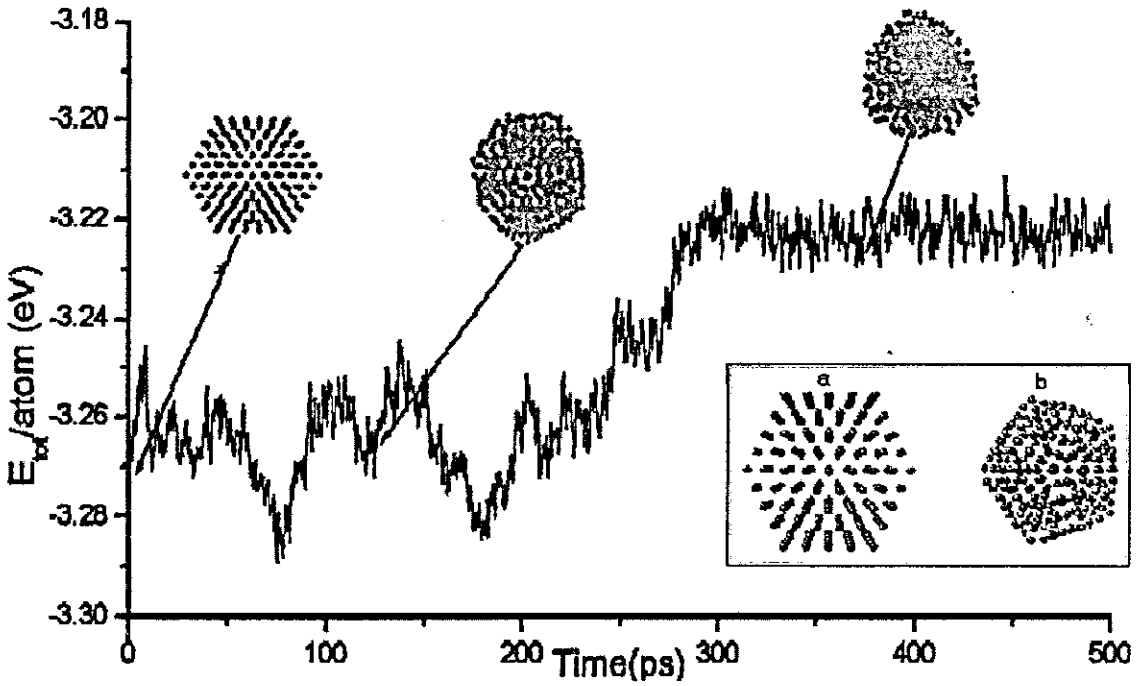

شكل (1):التغيرات التي تطرأ علي الطاقة الكلية للذرة مع الزمن لعنقود البلاديوم ذو ال561 ذرة على درجة الذوبان (1100K) كما يظهر التغير البنائي للعنقود على طول هذه الفترة و في الزاوية يظهر عنقود البلاديوم ذو 309 ذرات قبل و بعد تحوله من البناء[a]Cuboctahedral إلى البناء[b]Icosahedral.

4. عناقيد البلاديوم ذات الأعداد السحرية(Magic Number Palladium Clusters) هي أكثر اتزانا و ثباتا (More Stable) و تحتاج إلى وقت أطول للانصهار من تلك الأصغر أو الأكبر قليلا و التي لا تحوي أعدادا سحرية من الذرات على نفس درجة الانصهار.

5. العنقود ذو البناء (Icosahedron) هو أيضا أكثر اتزانا و ثباتا من العنقود ذو البناء(Cuboctahedron) بالرغم من كون البناءين ذوا أعداد سحرية من الذرات.

6. لوحظ تباين بين درجتي حرارة التحول للعنقود عند صهر العنقود و عند تبريد العنقود المنصهر.

7. العناقيد ذات الأحجام الصغيرة جدا لها درجات انصهار عالية جدا، تم بحث هذه الصفة للعنقود ذو الثلاث عشرة ذرة من البلاديوم.

و أخيرا فان نتائج هذه الأطروحة تتوافق مع نتائج البحوث الخاصة بعناقيد المعادن بشكل عام، و توضح الخصائص المرافقة لعملية الانصهار لعناقيد البلاديوم ذات الأعداد السحرية بشكل خاص.

معاني المصطلحات
Glossary

Cluster عنقود أو تجمع من الذرات

Molecular Dynamics Simulation المحاكاة لديناميكيات الجزيئات

Embedded atom potential جهد الذرة المطمورة أو المدفونة

Molecular simulation المحاكاة الجزيئية

Magic Numbers الأعداد السحرية

The Bulk الكتلة

Latent Energy of Fusion الطاقة الكامنة للانصهار

More Stable أكثر اتزانا و ثباتا